

Colloquium 2016: Assessment of the subsurface thermal conductivity for geothermal applications

Jasmin Raymond

*Institut national de la recherche scientifique, Centre Eau Terre Environnement, 490 de la
Couronne, Québec (Québec) Canada G1K 9A9
jasmin.raymond@inrs.ca; T: +1 418 654 2559; F: + 1 418 654 2600*

Abstract

The construction of green buildings using geothermal energy requires knowledge of the ground thermal conductivity, assessed when designing the heating and cooling system of commercial buildings with ground-coupled heat pumps. The most commonly used method for active field assessment is the thermal response test (TRT), which consists of circulating heated water in a pilot ground heat exchanger (GHE) where temperature and flow rate are monitored. The transient thermal perturbation is analyzed to evaluate the subsurface thermal conductivity. Heat injection can also be performed with a heating cable in the GHE to conduct a TRT without water circulation, which can be affected by surface temperature variations. Passive methods, such as the interpretation of geophysical well logs and the analysis of temperature profiles measured in exploration wells, are emerging as alternatives to TRTs. Steady-state and transient laboratory measurements performed on samples collected in surface outcrops or drill cores can also be achieved. Methods to characterize the subsurface in the context of geothermal system design have greatly evolved since the original TRT concept proposed during the 1980s with different techniques inspired from the Earth science sector.

Key Words: geothermal, geothermics, thermal geophysics, heat pump, thermal conductivity, thermal response test, ground heat exchanger.

Résumé

La construction des bâtiments verts qui utilisent l'énergie géothermique nécessite une connaissance de la conductivité thermique du sous-sol, évaluée lors de la conception d'un système de chauffage et de climatisation d'un bâtiment commercial munis de pompes à chaleur couplées au sol. La méthode la plus utilisée pour une évaluation active sur le terrain est celle du test de réponse thermique (TRT), laquelle consiste à faire circuler dans un échangeur de chaleur au sol (ECS) pilote de l'eau réchauffée où sont mesurés la température et le débit de circulation. La perturbation thermique transitoire est analysée afin d'évaluer la

conductivité thermique de la sous-surface. L'injection de chaleur peut également être effectuée à l'aide d'un câble chauffant inséré dans l'ECS pour réaliser le TRT sans circulation d'eau, celle-ci pouvant être affectée par les variations de température en surface. Des méthodes passives, comme l'interprétation des diagraphies de forage et l'analyse d'un profil de température mesuré dans un forage exploratoire, émergent maintenant en guise d'alternative aux TRT. Des mesures de laboratoire, en régime permanent ou transitoire, effectuées sur des échantillons, provenant d'affleurements ou de carottes de forage, peuvent finalement être envisagées. Les méthodes de caractérisation de la sous-surface utilisées dans un contexte de conception des systèmes géothermiques ont grandement évoluées depuis le concept original du TRT proposé durant les années 1980 avec différentes techniques inspirées du secteur des sciences de la Terre.

Mots-clés : géothermie, géothermique, géophysique thermique, pompe à chaleur, conductivité thermique, test de réponse thermique, échangeur de chaleur au sol.

Introduction

Geothermal heat pump systems, also named ground source heat pumps (Omer 2008), have become an important component of the living environment, tying buildings to the subsurface. The thermodynamic cycle of the heat pump involves extracting or injecting heat from or into the underground and transferring this thermal energy to or from the building to efficiently heat and cool indoor spaces. The system is installed in the subsurface having a low temperature, typically 6 to 10 °C for southern Canadian latitudes (Majorowicz et al. 2009), and benefits from the thermal inertia of the ground to heat and cool surface spaces subject to atmospheric temperature variations. Energy is required to drive the heat pump cycle through a compressor and the operation of the system results in energy savings, commonly 50~70 % of the energy consumed for heating and cooling with conventional technologies. Geothermal heat pumps replacing fossil fuel systems further contribute to the reduction of CO₂ emissions, thereby greening building operations (Canadian GeoExchange Coalition 2010).

Three main components constitute the systems, which are the building heating and cooling network, the heat pump and the ground heat exchangers (GHE; Florides and Kalogirou 2007). While many configurations using ground or surface water are possible for the latter, the Canadian market shows a strong preference for closed-loop GHEs totalizing more than 80 % of the system installed (Canadian GeoExchange Coalition 2012). Possible factors affecting user choices are lowest maintenance and environmental regulations associated with closed-loop systems, which are referred as a ground-coupled heat pumps (GCHPs; ASHRAE 2015). In that case, GHEs are most commonly made of high-density polyethylene pipes buried in boreholes or trenches. A heat carrier fluid, made of water and antifreeze, circulates through the pipe allowing heat exchange with the subsurface. The pipe can be surrounded by grout, sand or water for GHEs installed in boreholes or backfilled material in the case of trenches. Vertical GHEs installed in 100 to 200 m deep boreholes with a 10 to 15 cm diameter are popular for commercial size buildings, where limited surface space reduces the possibility of horizontal GHEs in shallow trenches of 1 to 2 m depth. Single and double U-pipes, as well as concentric pipes, are configurations used for the closed-loop GHEs (Raymond et al. 2015b). Beyond the GHE configurations, heat pump characteristics and building energy needs, the performance of such systems depends on the subsurface heat transfer ability. Heat conduction and storage are the dominant mechanisms taking place under low groundwater flow conditions, typically for a specific groundwater flux lower than $1 \times 10^{-6} \text{ m s}^{-1}$ to $1 \times 10^{-8} \text{ m s}^{-1}$ (Signorelli et al. 2007, Dehkordi and Schincariol 2014, Ferguson 2015).

Assessing the thermal state and properties of the subsurface, which impact the GHE's operating temperature and performances, is a critical task to design a GCHP system. Information about the undisturbed subsurface temperature, heat capacity and thermal conductivity until the planned GHE depth is needed to properly design a system. Those three input parameters are used to calculate the total length of borehole required to fulfill the energy needs of a building (Bernier 2000) and to simulate the GHE water temperature to evaluate possible energy savings (Bernier 2001).

The undisturbed subsurface temperature can be inferred from maps of the shallow subsurface temperature interpolated between boreholes (Majorowicz et al. 2009) or deduced according to atmospheric temperature data (Signorelli and Kohl 2004) using different analytical (Williams and Gold 1976) or empirical approaches (Badache et al. 2016). A direct measurement of a temperature profile in a pilot GHE is an additional option to reduce uncertainty when designing a GCHP system (Gehlin and Nordell 2003). The difference between predicted and observed subsurface temperature can be important in urban areas, where the built environment warms the ground through a phenomenon known as the urban heat island effect (Ferguson and Woodbury 2004; Zhu et al. 2010).

The subsurface heat capacity typically has a small variability among geological materials (Clauser 2014a). The sensitivity of geothermal system simulations with respect to heat storage is additionally less than that of conductive heat transfer and variability can be tolerated for the estimation of the subsurface heat capacity. The ability of geological materials to store heat is influenced by minerals, porosity and fluid content (Waples and Waples 2004a, 2004b), such that heat capacity can be estimated with appropriate knowledge of the subsurface deduced from geological maps, well log records and drill core or cuttings from an exploration well on site.

The remaining parameter with more challenges to evaluate when characterizing the subsurface to design a GCHP system is the thermal conductivity. This property describes the ability of a substance to transport heat through conduction mechanisms and varies among geological materials from 0.5 to $8 \text{ W m}^{-1} \text{ K}^{-1}$ (Clauser 2014b). The sensitivity of geothermal system simulations with respect to conductive heat transfer is high. For example, the length of borehole required to fulfill the energy needs of a building can increase by more than 50 % for geological materials with a low subsurface thermal conductivity below $2 \text{ W m}^{-1} \text{ K}^{-1}$ when compared to a high thermal conductivity above $6 \text{ W m}^{-1} \text{ K}^{-1}$ (Raymond et al. 2017c). Increasing the total length of boreholes can have a significant impact on the installation cost

of a GCHP system. Such design calculations are performed with the objective of minimizing the front cost to decrease the payback period when energy savings can cover the initial investment, making the GCHP system attractive and economically competitive.

The different methods to assess the subsurface thermal conductivity in the scope of geothermal heat pump system design are presented in this manuscript, with the objective of reviewing the current state-of-the art and research trends. GCHP design basics are initially covered and followed by a description of the thermal response test (TRT; Rainieri et al. 2011; Raymond et al. 2011; Spitler and Gehlin 2015), the most common field method to evaluate the subsurface thermal conductivity when designing a system. Alternative methods using a heating cable (Raymond et al. 2010, 2015a), geophysical well logs (Alonso-Sánchez et al. 2012), temperature profiles (Rohner et al. 2005; Raymond et al. 2016) and laboratory measurements (Luo et al. 2016a) are further described. An original classification is proposed to distinguish active vs passive, field vs laboratory, and steady-state vs transient methods. Illustrative examples of subsurface thermal conductivity assessments in the St. Lawrence Lowlands geological province are given at the sample to borehole scale for regional to site evaluation. The manuscript focuses on different techniques inspired from the Earth science sector and available to assess the subsurface thermal conductivity for geothermal applications, distinguishing from previous TRT reviews focusing on analytical methods (Rainieri et al. 2011; Raymond et al. 2011b; Zhang et al. 2014; Luo et al. 2016b) and an additional historical review describing scientific and commercial developments of TRT apparatus (Spitler and Gehlin 2015).

Historical perspective

The assessment of thermal conductivity in the scope of geothermal heat pump design is a relatively new field starting in the 1980s with the development of the original TRT concept (Mogensen 1983), a field experiment involving underground heat transfer at the scale of a GHE. Heat transfer theories to evaluate the thermal conductivity of geological materials are, however, much older and have recently been adapted to the geothermal heat pump environment enclosing the subsurface and the GHEs. Current scientific innovations in this field are commonly the result of technological adaptation rather than fundamental knowledge development dating back from the nineteenth century. It began with Fourier (1822) who defined the conductive heat transfer law from which analytical solutions were later derived, including the Kelvin line source theory further studied for quantitative geological applications into the 30s (Theis 1935; Carslaw 1945; Ingersoll et al. 1954). The father of quantitative

hydrogeology, Theis, adapted the infinite line source equation with the analogy between Fourier's and Darcy's law to describe the hydraulic response caused by pumping groundwater in an aquifer (Theis 1935). The theory is now widely used to infer the hydraulic conductivity of a confined aquifer subject to a perturbation of the hydraulic equilibrium. At the same time, it defines an approach that can be followed for in situ evaluation of other properties related to physical laws of the same form, like in the assessment of thermal conductivity with a TRT. First attempts to quantify the Earth's natural heat flux were achieved at the same period (Anderson 1934; Benfield 1939), a work that involved the assessment of the subsurface thermal conductivity. Heat flow modellers further contributed to the development of methods to evaluate the thermal conductivity of geological materials in the mid twentieth century. For example, Beck reported the development of laboratory (Beck 1957) and in situ methods (Beck et al. 1971) to evaluate the thermal conductivity of rocks and even worked on stratigraphic assessment from temperature profiles in boreholes (Beck 1976). Scientists, trying to estimate sea floor heat flow and understand plate tectonics, additionally made valuable contributions to the field of thermal conductivity evaluation such as Lister (1979), describing a method to evaluate thermal conductivity from the temperature decay following a heat pulse of a cylindrical source. Fundamental knowledge developed at this time constitutes the basis of modern thermal conductivity assessment methods that have been adapted to GHEs, with recent interest to solve geothermal heat pump problems. GCHP are complex systems designed according to ground thermal behaviour, with characterization methods that are now diversified and have been specifically developed to improve system performance.

GCHP design basics

When designing a geothermal heat pump system (Figure 1), the length, number and spacing of boreholes needed to maintain a minimum GHE water temperature during a given time period is calculated according to the building's energy needs, the subsurface thermal state and properties as well as the borehole configuration. The goal is to minimize the borehole length, or optimize the underground part of the system shown in Figure 1, to constrain the system cost and to ensure a compatible operating GHE temperature to achieve energy savings that will benefit the building operation. The heat pump coefficient of performance (COP), and therefore the energy savings that the system can provide, depends on the entering water temperature and flow rate (Figure 2). A low GHE temperature below the freezing point of water can result in a small borehole length but less energy savings. The art of GCHP design consists of finding a profitable trade-off between borehole length and energy savings.

Thermal energy is extracted from the ground by circulating a water solution with a temperature lower than that of the ground. Heat is transferred from the water solution of ground loop at the refrigerant-to-water heat exchanger (1) where the low pressure mix of vapour and liquid refrigerant evaporates. The refrigerant pressure is increased at the compressor (2) requiring an energy input, and the high-pressure vapour refrigerant transfers its thermal energy to the building air loop at the refrigerant-to-air heat exchanger (3). The refrigerant at high pressure condenses to liquid and the pressure is decreased at the expansion valve (4) to complete the heat pump cycle, which can be reversed for cooling mode operation.

A common approach is to calculate the length of borehole needed according to the building thermal loads transferred to the subsurface and the desired GHE water temperature affecting the heat pump COP. The building heating and cooling loads are defined as the thermal power needed to maintain a given indoor temperature. The loads imposed to the subsurface are calculated as a function of the building loads and the COP, and are named the ground loads. A part of the building loads are applied to the GHE field to reduce peak loads and maximize the GHE operation for hybrid systems combining geothermal heat pumps with other heating or cooling technologies (Hackel et al. 2009; Hackel and Pertzborn 2011). Various heat pulse schemes are used to simplify the ground loads with average monthly heat loads superimposed on peak loads (Eskilson 1987) or average yearly loads superimposed on average monthly loads of the design month and peak hourly loads (Bernier 2000; ASHRAE 2015). The design month is the coldest or the hottest month of the year, when building loads are most important, such that the design calculation can be carried out for heating and cooling conditions. The length of borehole L_b (m) needed to fulfill the building energy needs, for example, during a ten-year period under the last heat pulse scheme and assuming six hours for peak load duration in heating conditions, can be found with (Bernier 2000; Philippe et al. 2010):

$$L_b = \frac{Q_{10yr}R_{s,10yr} + Q_{1m}R_{s,1m} + Q_{6h}(R_{s,6h} + R_b)}{T_0 - \bar{T}_w + T_{pen}} \quad [1]$$

where Q (W) is the ground load and is positive for ground heat extraction. Both the ground loads and the subsurface thermal resistances R_s (m K W^{-1}) are calculated for a ten-year pulse (10yr) defined with average yearly loads, a one-month pulse (1m) defined with the average monthly load of the design month and a six-hour pulse (6h) defined with peak loads. The term R_b (m K W^{-1}) is for the borehole thermal resistance affected by the selected GHE configuration (Lamarche et al. 2010). The temperatures in the denominator are for T_0 (K), the

undisturbed subsurface, \bar{T}_w (K), the water in the GHE chosen for the design calculation, and T_{pen} (K), a penalty due to closely spaced boreholes. The average water temperature in the GHE for the heating mode is typically selected to be 6 to 11 °C smaller than the undisturbed subsurface temperature (ASHRAE 2015). Subsurface resistances are evaluated according to the temperature difference between the far field temperature and that at the GHE and the ground interface or the borehole radius. A thermal response function representing the GHE is used to calculate the temperature at the borehole radius like the infinite cylindrical heat source, the infinite line source or the finite line source equations (Philippe et al. 2009). The temperature penalty can be found according to the length, the separating distance and the disposition of boreholes in a given GHE field (Bernier et al. 2008) or removed from equation 1 and incorporated in the thermal response function representing the GHE with the superposition principle (Eskilson 1987).

A common approach to evaluate the subsurface thermal resistances in equation 1 is to use the infinite cylindrical heat source equation (Ingersoll et al. 1954):

$$R_{s,6h} = \frac{1}{\lambda_s} G_{ICS}(\tilde{r}, Fo_{6h}) \quad [2]$$

$$R_{s,1m} = \frac{1}{\lambda_s} [G_{ICS}(\tilde{r}, Fo_{1m+6h}) - G_{ICS}(\tilde{r}, Fo_{6h})] \quad [3]$$

$$R_{s,10y} = \frac{1}{\lambda_s} [G_{ICS}(\tilde{r}, Fo_{10y+1m+6h}) - G_{ICS}(\tilde{r}, Fo_{1m+6h})] \quad [4]$$

$$\tilde{r} = \frac{r}{r_b} \quad [5]$$

and

$$Fo = \frac{\alpha_s t}{r_b^2} \quad [6]$$

Resistances in equations 2 to 4 are a function of the subsurface thermal conductivity λ_s (W m⁻¹ K⁻¹) and the infinite cylindrical heat source equation G_{ICS} (-). The latter is a function of the normalized radius \tilde{r} (-), defined in equation 5 by the radial distance r (m) at which temperature is calculated and the borehole radius r_b (m), as well as the Fourier number defined with the subsurface thermal diffusivity α_s (m² s⁻¹) and the borehole radius in equation 6. The radial distance at which temperature is calculated to find subsurface resistances is the borehole radius such that the normalized radius in eq. 5 becomes unity. The response function G_{ICS} is a complex integral that can be approximated with tabulated values or curved fitted expressions (Kavanaugh and Rafferty 2014; Bernier 2000). The thermal state

and properties of the subsurface have a major impact on the borehole length calculated for design purposes, as evidenced by the undisturbed temperature and thermal conductivity of the subsurface in the denominator of equation 1 and equations 2 to 4, respectively.

The temperature of water in a GHE field can be simulated once a borehole length has been identified to confirm the GCHP design. The idea is to anticipate the GCHP operation and evaluate energy savings from the heat pump COP that is dependent on the entering water temperature (Figure 2). Thermal response functions are used to evaluate the average water temperature circulating in the GHE during heat pluses that are superimposed with respect to time. The equation to calculate average water temperature increments ($\overline{\Delta T_w} = \overline{T_w} - T_0$) for a period of constant heat injection rate takes the following form:

$$\overline{\Delta T_w}(t) = -\frac{q}{\lambda_s} G_{\text{ICS}}(\tilde{r}, Fo) - qR_b \quad [7]$$

where q (W/m) is the heat transfer rate per unit length of borehole and is positive for heat extraction. Various thermal response functions G can again be used in equation 7 and have different validity ranges (Philippe et al. 2009). The borehole thermal resistance R_b is to link the temperature at the borehole radius, calculated with the G function, to the water temperature in pipe assuming steady-state heat transfer inside the borehole. This global parameter includes the thermal resistances of the pipe and borehole filling materials in addition to that of the water flow in the pipe and can be calculated with empirical or analytical approaches (Remund 1999; Claesson and Hellström 2011). The important point here is to understand the impact of the subsurface thermal conductivity in the GCHP design and simulation process. Knowledge of the subsurface thermal conductivity allows reducing the risk of failure associated with GCHP operations. The risk is more important with multi-residential, commercial, institutional and industrial buildings having larger heating and cooling loads than single residential houses such that measurement of the subsurface thermal conductivity becomes critical for large buildings.

Methods to assess subsurface thermal conductivity

Thermal conductivity cannot be measured explicitly or directly. This property is evaluated from the analysis of temperature measurements during heat transfer experiments. Any such experiment involving the monitoring of temperature and heat transfer rate is referred to here as an active method to estimate the subsurface thermal conductivity (Table 1). TRTs are active transient methods performed in the field at the scale of a borehole with different methodologies. On the other hand, passive methods rely on a signal that does not involve heat

injection or extraction experiments, and can be interpreted to calculate the thermal conductivity. The analyses of geophysical well logs or a temperature profile measured in a borehole undisturbed by a TRT can be classified as a passive field method. Laboratory methods of interest are all active and conducted at the scale of a sample. Both transient and steady-state heat transfer experiments can be carried out to assess the thermal conductivity of the subsurface at the sample scale.

Active field methods

The most popular active field method to evaluate the subsurface thermal conductivity in the scope of geothermal system design is the TRT (Figure 3). It consists of injecting or extracting heat from the subsurface through an exploration borehole to disturb the subsurface thermal equilibrium and infer the thermal conductivity from the analysis of the temperature perturbation. The method is analogous to a pumping test where hydraulic equilibrium in an aquifer is disturbed by pumping the ground water to infer the hydraulic conductivity from the analysis of the water pressure perturbation (Raymond et al. 2011b). The theoretical concept of using a GHE as a heat source to infer the subsurface thermal conductivity was first proposed by Mogensen (1983), followed by full-scale tests enclosing all GHEs of a bore field to verify system performances as outlined by Spitler and Gehlin (2015). Mobile apparatus were developed later in 1995 in the United States and Sweden to perform tests in a single pilot GHE (Austin III 1998; Gehlin 1998). The development of TRT, which coincides with an increased interest in geothermal heat pumps during the energy crisis of the 1980's (Spitler and Gehlin 2015), is much younger than the development of pumping tests beginning with Theis's (1935) original theory. Now, TRTs are commonly carried out before the installation of the complete bore field through a pilot GHE that is later integrated to the complete GCHP system as design and installation proceed. The conventional method, where heat is injected underground at a constant rate by circulating heated water in a GHE where inlet and outlet temperatures are monitored, has evolved with alternative methodologies. Heat extraction tests, thermal recovery monitoring following heat injection, constant inlet temperature, temperature monitoring inside borehole and downhole heating cable tests are alternatives or modifications to the original method.

Conventional TRT

Electric heating elements at the surface are used to heat water circulating in the GHE during a conventional TRT. The heat injection rate shall be kept constant, although power fluctuations can affect heat generated with the electric elements. Atmospheric temperature fluctuations, wind speed and solar radiation can further affect the heat injection rate, which can be minimized with proper insulation of surface piping and TRT equipment (Kavanaugh 2001). The test starts with heat injection after purging air trapped in the GHE and circulating unheated water to measure the undisturbed subsurface temperature (Gehlin and Nordell 2003). North American guidelines suggest a heat injection rate of 50 to 80 W per metre of borehole, resulting in a 7.6 to 12.2 kW power for a typical 152 m long GHE (Kavanaugh 2001). The idea is to reproduce the GHE operation and create a temperature difference of 3 to 7 °C between the inlet and outlet of the GHE. Such high power may not be available in the field or on construction sites, and energy during tests is often supplied with a fuel-fired generator having sufficient fuel storage capacity to run continuously for more than 48 hours. The duration of the heat injection has been subject to debates since shorter tests can be cheaper but likely underestimate the subsurface thermal conductivity (Beier and Smith 2003; ASHRAE 2015; Liu and Beier 2009; Raymond et al. 2011b). A heat injection period of 40 to 60 h is, however, generally accepted.

Water temperature at the inlet and outlet of the GHE is measured along with the flow rate during a TRT. This data is used to calculate for each measurement step the heat injection rate Q (W) according to:

$$Q = -Q'(T_{w,i} - T_{w,o})\rho_w c_w \quad [8]$$

where Q' ($\text{m}^3 \text{s}^{-1}$) is the flow rate, $T_{w,i}$ and $T_{w,o}$ (K) are the inlet and outlet water temperature, and $\rho_w c_w$ ($\text{J m}^{-3} \text{K}^{-1}$) is the water volumetric heat capacity. Measurements recorded every ten minutes or less can be averaged to find the mean heat injection rate. Inlet and outlet water temperatures are additionally averaged before being analyzed to evaluate the mean GHE water temperature:

$$\overline{\Delta T_w} = \frac{\overline{\Delta T_{w,i}} + \overline{\Delta T_{w,o}}}{2} \quad [9]$$

Evaluating the GHE water temperature with this arithmetic average implies a symmetrical temperature profile along the descending and ascending pipe of the GHE and a constant heat injection rate with depth along the borehole (Figure 4). Numerical simulations of GHE

temperature illustrated in Figure 4 has demonstrated that this condition is rarely met and alternative averages have been proposed to account for the asymmetric temperature profile along the descending and ascending pipes (Marcotte and Pasquier 2008; Beier et al. 2012). Marcotte and Pasquier's (2008) p-linear average has become popular and can be calculated with:

$$\overline{\Delta T_w} \approx |\Delta T_p| = \frac{p(|\overline{\Delta T_{w,i}}|^{p+1} - |\overline{\Delta T_{w,o}}|^{p+1})}{(1+p)(|\overline{\Delta T_{w,i}}|^p - |\overline{\Delta T_{w,o}}|^p)} \quad [10]$$

where p (-) is a fitting parameter that tends toward -1. Equation 10 is generally used when considering a 2D borehole thermal resistance. Thermal short circuiting between the GHE pipes can alternatively be taken into account by evaluating a 3D borehole thermal resistance considering the internal borehole thermal resistance as defined by Hellström (1991), which should be the case when using equation 9 (Lamarche et al. 2010).

The averaged water temperature increments can be reproduced analytically with a heat source function to find the subsurface thermal conductivity. The infinite line source equation (Carslaw 1945) has a validity range on the order of hours (Philippe et al. 2009) and is therefore suitable for TRT analysis, where computed temperature increments are found with:

$$\overline{\Delta T_w} = -\frac{q}{\lambda_s} G_{ILS}(Fo) - qR_b \quad [11]$$

For $Fo > 5$, the infinite line source function G_{ILS} (-) can be approximated with:

$$G_{ILS}(Fo) = \frac{1}{4\pi} [\ln(4Fo) - \gamma] \quad [12]$$

where $\gamma = 0.5772\dots$, which is Euler's constant. Developing equation 11, it follows that:

$$\overline{\Delta T_w} = -q \left[\frac{1}{4\pi\lambda_s} \left(\ln \left(\frac{4\alpha_s t}{r_b^2} \right) - \gamma \right) + R_b \right] \quad [13]$$

Equation 13 has a linear form $Y = m \cdot X + b$, where the slope m ($K s^{-1}$) is:

$$m = -\frac{q}{4\pi\lambda_s} \quad [14]$$

and the intercept b (K) is:

$$b = -q \left[\left(\frac{\ln \left(\frac{4\alpha_s}{r_b^2} \right) - \gamma}{4\pi\lambda_s} \right) + R_b \right] \quad [15]$$

Two options are then possible to analyze a TRT: 1) observed temperature increments can be fitted to computed temperature increments with equation 11 adjusting unknown parameters

manually or using a non-linear solver (Wagner and Clauser 2005; Raymond et al. 2011b; Bozzoli et al. 2011; Pasquier 2015); 2) observed temperature increments can be plotted as a function of logarithmic time to calculate the subsurface thermal conductivity with the slope from equation 14 (Sanner et al. 2005) and the borehole thermal resistance from the intercept with equation 15 (Beier and Smith 2002). For the first option or the calculation of the thermal resistance with the second option, the analysis requires an estimation of the subsurface volumetric heat capacity that can be found with rock or unconsolidated sediment type in order to calculate the thermal diffusivity when necessary. The curve-fitting approach with the first option is an ill-posed problem as more than one combination of the subsurface thermal conductivity and the borehole thermal resistance can generate similar temperature solutions. The calculation of the borehole thermal resistance with equation 15 depends on the subsurface thermal conductivity previously found with equation 14. In any case, the borehole thermal resistance can be constrained from various analytical and empirical methods to calculate the resistance from the GHE configuration and materials (Lamarche et al. 2010).

The infinite line source equation modified by Theis (1935) with the analogy of heat transfer to porous media flow demonstrates the link between TRT and pumping test analysis. The approximation made to the infinite line source equation for $Fo > 5$ in equation 12 is equivalent to Cooper and Jacob's (1946) method to compute drawdown during a pumping test. The second parenthesis term on the right-hand side of equation 13 is equivalent to a well function in pumping test analysis and the borehole thermal resistance is equivalent to the skin factor divided by $2, \pi$ and the subsurface thermal conductivity (Raymond and Lamarche 2013). TRT analysis is somewhat similar to pumping test analysis in confined aquifers except that, for economic reasons, TRTs are carried out with a single borehole while pumping tests can involve several observation wells. This allows the specific storage of the aquifer to be evaluated, whereas the subsurface specific heat capacity cannot be identified with a TRT. Similarly, this is the case of single well hydraulic tests such as packer and drill stem tests, allowing the determination of transmissivity only. Subsurface heat transfer processes involved in this conventional TRT are obviously transient as subsurface and GHE temperatures keep changing as heat injection proceeds during this field experiment.

Alternatives to the conventional TRT

Field alternatives to the conventional heat injection TRT, using a mobile unit with a pump and electric heating elements at the surface, have evolved with modifications proposed to the equipment to run the test or do field manipulations itself.

Heat extraction TRT

The electric heating elements in a TRT unit can be replaced by a heat pump to run the test in heat extraction mode (Witte et al. 2002; Rolando et al. 2017). An air source heat pump is used, but the heat extraction rate can be subject to fluctuations, which can be minimized by installing a water reservoir and proper control valves in the TRT unit. Overall, the test can be used to evaluate subsurface properties under low GHE temperature to reproduce conditions triggered by a heat pump during the heating season of a building.

Downhole temperature measurements

Combining the conventional TRT apparatus with distributed temperature-sensing technology using fiber optic cables to measure temperature (Siska et al. 2016) at depth was initially achieved by Fujii et al. (2006), followed by other researchers (Fujii et al. 2009; Acuña et al. 2011; Acuña and Palm 2013; Holmberg et al. 2016). The fiber optic cable is installed in the GHE inside or outside the pipe. Temperature variations along the fiber optic affect the capacity of the cable to transmit light. A laser signal sent to the cable interacts with the silica molecules of the fiber optic excited by the temperature perturbation and diffuses the light returning with a phase shift under the Raman effect. The returning laser signal allows temperature to be evaluated along the fiber optic cable. The spatial resolution of temperature measurements can be less than one metre. The temperature signal at each depth is analyzed to find a thermal conductivity profile along the GHE rather than a bulk value representative of the GHE depth when compared to the conventional TRT. The analysis of the temperature signal at each depth can be achieved with an analytical solution, commonly the infinite cylindrical heat source (eq. 7) or the infinite line source functions (eq. 11), assuming that heat transfer is dominantly perpendicular to the GHE and that vertical or axial heat transfer among subsurface slices is negligible (Fujii et al. 2009). The unit to read and record temperature along a fiber optic cable can be expensive and TRT with similar temperature measurement at depth can be carried out with submersible data loggers enclosing a temperature sensor or with a chain of thermistors but with a large spatial resolution. The idea of using a single flowing

water sensor travelling along the GHE and recording the temperature at different depths has been tested further (Martos et al. 2011).

Monitoring of the thermal recovery

An alternative manipulation that can be achieved without modification of the conventional TRT unit is the monitoring of the thermal recovery period following heat injection (Raymond et al. 2011b, 2011a). This can be performed in two different ways: 1) the water can be kept flowing in the GHE after heat injection is stopped, water temperature is recorded at the inlet and outlet of the GHE until it returns near initial conditions; 2) alternatively, the water circulation along the GHE can be stopped at the same time as the heat injection, and the temperature is recorded inside the GHE with fiber optics, data loggers, thermistors or other submersible devices. The first method is to find a bulk thermal conductivity based on recovery measurement analysis while the second is to evaluate thermal conductivity at distinct depths. Another alternative is to compare thermal conductivity estimates obtained from the analysis of heat injection and recovery data. The analysis of both global and local temperature measurements during the recovery period can be done by applying the temporal superposition principle to a heat source function. Under variable heat injection rates, equation 11 becomes:

$$\overline{\Delta T}_w = \frac{-1}{\lambda_s} \sum_{i=1}^N (q_i - q_{i-1}) G_{ILS}(Fo_i) - q_i R_b \quad [16]$$

$$\text{where } Fo_i = \frac{\alpha_s(t-t_{i-1})}{r_b^2} \quad [17]$$

During the recovery period preceding a test with a constant heat transfer rate equal to q , the water temperature increments can be calculated with

$$\overline{\Delta T}_w = -\frac{q}{\lambda_s} [G_{ILS}(Fo) - G_{ILS}(Fo_{off})] \quad [18]$$

where Fo_{off} is calculated according to the recovery time ($t-t_{off}$) for which t_{off} is when the heat injection stopped. The borehole thermal resistance is cancelled from equation 18 because the heat injection rate is assumed to be zero during the recovery period. Numerical simulations of the temperature distribution in a slice of borehole during a TRT showed that temperature becomes uniform shortly after heat injection stops (Figure 5; Raymond et al. 2011a), evidencing the negligible effect of the borehole thermal resistance as temperature recovery proceeds. The temperature gradient across the borehole is illustrated to be less than 1 °C five hours after the end of heat injection while it was more than 5 °C at the end of heat injection.

For $Fo_{\text{off}} > 5$, the water temperature increments during the recovery period can be estimated with:

$$\overline{\Delta T}_w = \frac{-q}{4\pi\lambda_s} \left[\ln \left(\frac{4\alpha_s \left(\frac{t}{t-t_{\text{off}}} \right)}{r_b^2} \right) \right] \quad [19]$$

Equation 19 has a linear form $Y = \tilde{m} \cdot X + b$, where the slope \tilde{m} (K s^{-1}) is defined according to the normalized time $\tilde{t} = [t/(t-t_{\text{off}})]$ and can be used to calculate the thermal conductivity:

$$\tilde{m} = -\frac{q}{4\pi\lambda_s} \quad [20]$$

Temperature measurements recorded during the recovery period can be analyzed in a similar fashion than temperature increments of the heat injection period. Temperature observations are reproduced using either curve-fitting procedures with equation 18, or the slope method (equation 20) for which observed temperatures are plotted as a function of normalized logarithmic time. Late recovery temperature increments tend to become independent of the borehole thermal resistance such that this parameter is found with heat injection data after finding the subsurface thermal conductivity with recovery data. The effective duration of the heat injection period of a TRT can additionally be extended using temperature measured during the recovery (Raymond et al. 2011b), following the methodology developed to extend pumping tests (Neville and van der Kamp 2012).

TRT with a heating cable

A reinvented TRT method relies on a heating cable installed in the borehole to inject heat underground (Raymond et al. 2010, 2015a). Such tests were initially done in boreholes filled with groundwater for hydrogeological purposes (Pehme et al. 2007) and have been adapted to GHE in the context of geothermal system design. Water is not flowing in the GHE and the cable is installed in the standing water column filling the GHE pipe with temperature sensors tied to the cable (Figure 6). The heat injection rate is not affected by atmospheric temperature variations and solar radiation in opposition to conventional TRT where surface processes can affect the heat injection rate. The heating cable can be continuous or composed of short heating sections of 1 to 2 m in length separated by non-heating sections of greater length. The idea here is to minimize the heat injection rate to perform the test with a low power source and avoid the need for a fuel-fired generator to supply power with a high voltage. Tests with a heat injection rate of 15 to 30 W/m of borehole with a continuous cable in boreholes less than 50 m deep and with 10 to 15 heating sections in boreholes 100 to 150 m deep have been achieved with a power source of less than 1.2 kW. The heat injection rate in the case of

heating cable tests is adjusted to create sufficient temperature differential to be detected according to the resolution of the temperature sensors.

Analysis of heat injection data can be achieved with the slope method using equation 14 if the cable remains stable and does not move inside the borehole. A cable moving a few millimeters can result in an oscillatory temperature signal. Curve-fitting analysis of heat injection data can be difficult since the exact position of the temperature sensor with respect to the pipe or GHE section is unknown. The temperature around the cable for a given depth becomes uniform during the recovery period such that temperature curves measured at different horizontal positions all collapse together during the recovery period (Raymond et al. 2011a). Therefore, the analysis of recovery data can be achieved with either curve-fitting procedures using equation 18 or the slope method with equation 20. Infinite heat source solutions are unsuitable for analysis of TRT with heating sections that can be relatively short. A finite heat source solution must be used, similar to equation 18, but taking into account the finite length of heating sections (Raymond and Lamarche 2014). Recently, a new concept of combined hydro and thermal response tests was proposed with a heating cable and temperature sensors around the cable inside an open well to evaluate not only the subsurface thermal conductivity, but additionally the groundwater flow velocity and direction (Rouleau et al. 2016).

Constant temperature TRT

The TRT unit can be modified with proper control mechanisms and a water reservoir to inject fluid at a constant temperature and maintain a constant temperature differential of 3 to 7 °C between the inlet and outlet of the GHE (Wang et al. 2010). The average water temperature inside the GHE remains constant and the heat injection rate is adjusted to maintain the GHE fluid temperature. A water reservoir at the surface with temperature controlled by a heat pump is used to inject the water at a constant temperature such that tests can be carried under heat injection or extraction modes. Units without a water tank and a heat pump, including a solid-state relay and a general proportional–integral–derivative controller linked to electric heating elements, have further been proposed to simplify field operations in order to conduct tests with a constant water temperature (Choi and Ooka 2017). The analysis relies on an infinite line or cylindrical source solution derived for a constant temperature at the source radius, which is different from the boundary condition used for conventional TRT where a constant heat injection rate is assumed (Yu et al. 2016; Aydin et al. 2017). The constant-temperature TRT allows the test time to be reduced when compared to conventional TRT with constant

heat injection rate. The constant GHE temperature can be reached in less than 10 h while a period of at least 30 h is necessary to reach a constant GHE temperature increase needed for analysis with the conventional method.

TRT influenced by groundwater flow

Analyzing a TRT with the analytical solutions presented in this manuscript assumes that heat transfer between the GHE and the subsurface is dominantly affected by conduction. Groundwater flow can influence heat transfer and an effective thermal conductivity varying, for example, up to 16 % has been found for TRTs carried out under different groundwater flow conditions (Bozdağ et al. 2008). TRT with downhole temperature measurements analyzed with infinite line or cylindrical source equations can reveal zones of higher equivalent thermal conductivity that can be associated with groundwater flow if corresponding to fracture zones (Fujii et al. 2009). Peclet number analysis can be carried out to compute the groundwater flow velocity from the equivalent subsurface thermal conductivity perturbed by flow when comparing this value to the thermal conductivity of zones unaffected by flow (Lehr and Sass 2014). The analysis of a TRT affected by groundwater flow can further be conducted with a numerical model coupling groundwater flow and heat transfer taking into account advective and dispersive heat transfer (Signorelli et al. 2007; Raymond et al. 2011c). Information about the hydraulic gradient, conductivity and dispersivity prevailing in the subsurface must be known to achieve such analysis. An alternative to analyze the test is to use the spatial superposition principle with the infinite line source equation to simulate a moving heat source (Chiasson and O'Connell 2011; Molina-Giraldo et al. 2011; Wagner et al. 2013). The subsurface thermal conductivity can be inferred if information about groundwater flow velocity is known. This approach can consider an asymmetrical heat propagation around a GHE and is suited for conditions where Darcy flux is beyond $1 \times 10^{-6} \text{ m s}^{-1}$ to $1 \times 10^{-8} \text{ m s}^{-1}$ (Signorelli et al. 2007, Dehkordi and Schincariol 2014, Ferguson 2015).

Passive field methods

Geophysical methods to investigate subsurface conditions are now being used in the context of geothermal heat pump system design. The methods can help to characterize the subsurface with downhole acoustic and gamma ray logs to identify fractures and lithology (Radioti et al. 2016). Surface resistivity surveys have also been used to image the temperature perturbation of operating geothermal systems (Arato et al. 2015; Giordano et al. 2016). Of interest to this literature review is the interpretation of geophysical signals to evaluate the subsurface thermal conductivity that is classified as passive field methods. Surveys have so far been performed in

boreholes, which need to be open to complete well logs before installing the GHE pipe or can be carried out inside the pipe of the GHE in the case of temperature profile in equilibrium with subsurface temperature.

Geophysical well log

Wireline logging can measure the host rock response to various geophysical signals. Gamma ray log, measuring the natural radioactivity of the formation in American Petroleum Institute (API) units, is frequently used in sedimentary rocks to distinguish shale, commonly containing radioactive elements, from clean sandstone or limestone depleted of radioactive elements. In this context, Alonso-Sánchez et al. (2012) proposed that gamma ray signals be measured in a borehole before installing a GHE to determine the shale and limestone fraction and calculate the resulting thermal conductivity. Drill cuttings were sampled and analyzed in the laboratory to determine the thermal conductivity of the shale and limestone to constrain the calculation of thermal conductivity that was compared to that obtained with conventional TRTs. Despite the fact that very few studies have used geophysical well logs to evaluate the subsurface thermal conductivity in shallow boreholes of one to two hundred metres' depth, there are many methods available, most of which originate in kilometre-deep boreholes drilled for heat flow assessment or evaluation of geothermal resources with high temperature to generate electrical power. A review of the methods that have been used in the field of deep geothermal energy can consequently help envision which methods could be applied to shallow GHE in the near future.

Analytical and empirical approaches can be used to calculate thermal conductivity from geophysical well logs (Figure 7). The analytical approach consists of inverting well logs to find the mineral and porosity fraction of the host rock to calculate thermal conductivity with mixing models (Brigaud et al. 1990; Dove and Williams 1990; Demongodin et al. 1991; Vasseur et al. 1995; Midttømme et al. 1998). Many well log signals, commonly including gamma ray, density, neutron porosity, photoelectric factor and transit time, are needed to achieve the inversion and infer the mineralogical and porosity fractions of heterogeneous host rocks. The identified rock components are the basis to calculate the thermal conductivity with mixing models, commonly the arithmetic, geometric and harmonic averages (Clauser 2014b):

$$\lambda_{\max} = \lambda_{\text{ari}} = \sum_{i=1}^N n_i \lambda_i \quad [21]$$

$$\lambda_{\text{geo}} = \prod_{i=1}^N \lambda_i^{n_i} \quad [22]$$

$$\lambda_{\min} = \lambda_{\text{har}} = \left(\sum_{i=1}^N \frac{n_i}{\lambda_i} \right)^{-1} \quad [23]$$

where n (-) is the fraction of each component i of known thermal conductivity λ_i ($\text{W m}^{-1} \text{K}^{-1}$). The arithmetic average provides the maximum estimate and is representative of heat transfer parallel to a stratified medium while the harmonic average yields the lowest estimate characteristic of heat transfer perpendicular to a stratified medium. The geometric average is representative of a medium composed of angular fragments surrounded by fluid and often used because it provides an intermediate value having good correlation with measured thermal conductivity. The analytical approach to well log analysis is suitable with any rock type of any region, given that a combination of well logs can differentiate the main mineralogical phases of the host rock.

Empirical approaches can, on the other hand, directly relate a well log signal to thermal conductivity (Pribnow et al. 1993; Kukkonen and Peltoniemi 1998; Popov et al. 2003; Hartmann et al. 2005; Goutorbe et al. 2007; Sundberg et al. 2009; Gegenhuber and Schoen 2012; Fuchs and Förster 2013; Gasior and Przelaskowska 2014). Limited well logs signals can be used for that purpose. The relationships tying well log signals to host rock thermal conductivity are, however, limited to given rock types in specific regions since a universal empirical relationship is inexistent. Laboratory measurements of thermal conductivity on core or drill cutting samples are used to define the empirical relationships with respect to specific rock type. In the absence of significant drill core to derive statistically representative relationships, Nasr (2016) used the analytical approach with reference wells having log signals of good quality to infer empirical relationships and calculate the thermal conductivity with limited well log signals in a study of the St. Lawrence Lowlands deep geothermal resources. For example, it was determined that the thermal conductivity of Potsdam sandstone at the base of the sedimentary sequence can be calculated from gamma ray and neutron porosity logs with:

$$\lambda_{\text{Potsdam ss}} = 6.95 - 0.026 \cdot GR - 9.50 \cdot \theta \quad [24]$$

where GR (API) and θ (-) are the gamma ray and neutron porosity signals. Such a relationship can easily be applied to calculate the thermal conductivity when compared to all the efforts needed to complete an inversion to infer the mineralogy, but is limited to the given rock type in the St. Lawrence Lowlands sedimentary basin.

Temperature profile

The measurement of a temperature profile in a GHE undisturbed by heat injection or extraction experiments and in equilibrium with the subsurface temperature can provide a geophysical signal to analyze and infer the subsurface thermal conductivity. Variations of the geothermal gradient are characteristic of lithological changes, and temperature logs have been used for decades to help define stratigraphy (Beck 1976). The temperature measurement can be performed in the GHE pipe taking caution about the rise in water level that can be produced by inserting a probe in a closed loop. Rohner et al. (2005) developed a wireless submersible temperature and pressure probe that sinks down the GHE and is recovered by flushing the pipe with a pump. The depth is calculated from the pressure recordings and the disturbance to the water level is negligible since the probe is wireless. Alternatively, Raymond et al. (2016) proposed to use a wired pressure and temperature probe and compensate the depth for the rise in water level that can be measured before and after the temperature profiling.

The analysis of the temperature profile to calculate the subsurface thermal conductivity can be done with Fourier's Law of heat conduction, when knowing the Earth's heat flow to calculate the thermal conductivity from the geothermal gradient:

$$\lambda_s = q^* \frac{\Delta T}{\Delta z} \quad [25]$$

where the heat flow q^* (W m^{-2}) is negative toward the surface. This approach was verified by Rohner et al. (2005) with comparison to thermal conductivity measured in the laboratory on samples of cuttings, but worked for the deepest part of the borehole only, more than 50 m deep in that case. The reason for discrepancy near the surface is because the temperature profile can be affected by topography and paleoclimates (Kohl 1998, 1999). The method using equation 25 is limited to regions where the Earth's heat flow has been mapped with accuracy; for example, in areas where equilibrium temperature profiles and core thermal conductivity analysis have been completed in several deep wells. Deep equilibrium temperature measurements providing an accurate distribution of the Earth's heat flow in Canada are found in the Western Canadian Sedimentary Basin (Grasby et al. 2011). However, few heat flow assessments are not available for large cities in the Quebec-Windsor corridor of the St. Lawrence Lowlands where the installation of geothermal systems is most frequent.

In the absence of knowledge about the Earth's heat flow, Raymond et al. (2016) proposed using temperature profiling to extend the thermal conductivity assessment of a given GHE field beyond a first borehole, in which a TRT has been conducted. An inverse numerical

model simulating conductive heat transfer that takes into account topography and the recent rise in surface ground temperature attributed to climate warming has been developed to reproduce temperature profiles measured in two GHEs. The model was used to find the basal heat flow at the site by reproducing the temperature profile in the GHE where the TRT had been conducted. Assuming the same heat flow at the second GHE, the temperature profile was reproduced to find the bulk subsurface thermal conductivity at the location of the second GHE. Measuring a temperature profile in a GHE is a cheap alternative when compared to all the field operations needed for a conventional TRT. The analysis of temperature profiles can be fruitful provided that spatial limitations about knowledge of the Earth's heat flow, topography and paleoclimates can be addressed properly. Greater uncertainty due to variability of the Earth's heat flow and paleoclimates is expected when comparing such passive method to active TRT assessments. Passive evaluation of the subsurface thermal conductivity could further involve the analysis of temperature recorded for time series of shallow depth (Horton et al., 1983), but has not been extensively used for geothermal system design since it requires long monitoring that can exceed the time available to design a GCHP.

Laboratory methods

The laboratory analysis of thermal conductivity on samples of rock and unconsolidated deposits can be particularly useful in regional assessments mapping the subsurface thermal conductivity distribution to define the geothermal potential of a region (Di Sipio et al. 2014). Samples can be collected from outcrops and drill core to carry out the analysis in the laboratory. Such active methods can be classified according to the heat transfer state at which experimental work is conducted. Steady-state methods where heat transfer takes place across the whole sample can take into account the effect of the sample heterogeneity. The depth of penetration of transient methods where a heat pulse is applied to the sample is limited and the transient approaches are, consequently, better suited for homogeneous materials. There is a large variety of laboratory methods to evaluate the thermal conductivity at the sample scale; for example, those used with granular construction materials (Côté and Konrad 2005; Côté et al. 2013). The methods that have been used so far in the geothermal heat pump sector are described below.

Steady-state method

The divided bar method can be used to evaluate the thermal conductivity of core plug samples (Beck 1957; Beck and Beck 1958). A cylindrical sample ~1–2 cm thick is placed across a bar made of discs with high thermal conductivity, for example brass or copper, separated by discs of a reference material of known thermal conductivity on the same order of magnitude to that of the sample (Figure 8). Constant temperatures are maintained at the extremities of the bar with water circulating baths to ensure a steady heat transfer rate. The material of known thermal conductivity is to evaluate the heat flow across the bar. Fused quartz of thermal conductivity equal to $1.38 \text{ W m}^{-1} \text{ K}^{-1}$ is frequently used because the substance is relatively pure. Under steady-state temperature and negligible contact resistance, heat flow across the reference discs and the sample are given by:

$$q_{1-2} = -\lambda_{\text{ref}} \frac{T_2 - T_1}{H_{\text{ref}}} \approx q_{2-3} = -\lambda_{\text{sample}} \frac{T_2 - T_3}{H_{\text{sample}}} \approx q_{3-4} = -\lambda_{\text{ref}} \frac{T_3 - T_4}{H_{\text{ref}}} \quad [26]$$

where H (m) is the thickness of the sample and the reference (ref) material. The thermal conductivity of the sample can be found from equation 26 assuming that heat flow is constant across the bar. Thermal resistance at the sample contact can be taken into account to improve the accuracy of the measurements.

The surfaces of the sample to analyze are grinded to ensure uniform sample thickness and parallel faces. The flatness and parallelism of a sample should be within 0.03 mm and 0.1 mm, respectively. The sample preparation can be difficult when the rock is not well consolidated, as is sometimes the case with sandstone, or friable, which occurs with mudstone and shale. A thermal contact agent such as thermal grease can be applied to the sample surface to reduce contact resistances. Measurements can be performed on dry and saturated samples. About thirty minutes to more than one hour may be needed for the bar temperature to reach equilibrium, making the analysis time consuming. A technique has been developed to infer the heat capacity from the transient response before the bar temperature reaches equilibrium, allowing more information to be extracted during the analysis (Antriasian and Beardsmore 2014). The divided-bar method was used by Barry-Macaulay et al. (2013, 2014) to measure the thermal conductivity of dry and saturated sedimentary rock and basalt samples from the area of Melbourne, Australia. The work was performed to compile a database about subsurface thermal conductivity to help design geothermal heat pump systems.

Transient methods

Transient thermal conductivity analysis in the laboratory can be an alternative to the steady-state method with shorter analysis time and a sample preparation that is better adapted to unconsolidated or friable materials. The thermal conductivity evaluation is characteristic of the material at the sample interface in contact with the heat source. The different transient methods are generally named according to the form of the heat source (Figure 9).

The needle probe or hot wire is an elongated metallic heat source with an embedded temperature sensor to monitor temperature changes at the sample interface (Bristow and White 1994). The heat source has a relatively small radius with respect to its length such that the infinite line source equation can be used to analyze a test with curve-fitting procedures using equation 13 or the slope method using equation 14 to find the thermal conductivity upon radial heat injection. Thermal recovery can additionally be monitored and analyzed to evaluate the thermal conductivity with equations 19 and 20. A single analysis can be carried out within a few minutes. Thermal grease can be spread on the needle to ensure good contact with the sample. Drilling a thin hole in solid rock can be difficult but is feasible for a thicker needle adapted to solid materials. The needle probe method remains best suited for unconsolidated deposits. A heating line embedded into a block of poorly conducting material placed on a sample flat surface was alternatively developed (Vacquier 1985), which can facilitate analysis with rock samples. Dual needles are available, in which the second needle is used to monitor the temperature perturbation at a few centimetres from the first needle injecting heat. The thermal conductivity and diffusivity as well as the heat capacity can all be determined with the dual needle probe (Bristow et al. 1994).

The transient plane source method relies on a flat heating element sandwiched between two samples with surfaces that have been grinded to ensure flatness (Shabbir et al. 2000). A momentary constant heat pulse is transferred to the sample by applying a known current intensity to the heating element. The increase of temperature at the sample interface is analyzed to infer thermal properties. A modified transient plane source (MTPS) method was developed to facilitate analysis where a single face of the sample is placed on the heating element with reflectance allowing one-dimensional heat transfer (Harris et al. 2014). The change in potential difference across the heating element is measured with the modified plane source device and the thermal conductivity is inversely proportional to the rate of increase in potential difference used as a proxy for temperature. This experiment allows a measurement

of the thermal diffusivity that can be interpreted to determine thermal conductivity with proper calibration when knowing the range of heat capacity anticipated for the sample.

The preparation of samples for transient thermal conductivity analysis tends to be easier than that of steady-state since there is no need to have parallel upper and lower faces. This is especially true for the modified transient plane source method. Any sample shape with a flat surface where heat is injected can potentially be used, making the method more suitable for friable rocks, such as siltstone or shale. However, the heat pulse sent through the sample has a limited penetration depth on the order of a few millimetres and the transient measurement is representative of the material at the contact with the heating element only. Transient methods consequently tend to be more suitable for homogenous material while the steady-state divided bar method can take into account the sample heterogeneity because heat is transferred across the whole sample.

Transient laboratory methods have been used to evaluate the thermal conductivity of unconsolidated deposit and rock samples at the regional scale to help design GCHP systems. For example, Barry-Macaulay (2013, 2014) used the needle probe method to develop a database of the subsurface thermal conductivity in the area of Melbourne when dealing with unconsolidated deposits. Di Sipio et al. (2014) made use of both the needle probe and the MTPS methods to map the thermal conductivity of host rock and sedimentary deposits in Southern Italy. The assessments of laboratory samples provided the information needed to simulate geothermal heat pump systems and develop a geothermal potential map with geographic information systems (Galgaro et al. 2015). Luo et al. (2016a) additionally used the embedded needle probe method to compare thermal conductivity measurements at the sample to field scale with a TRT. A discrepancy was observed between laboratory and field results with higher thermal conductivity in the laboratory, suggesting a scale effect when assessing the thermal conductivity.

Illustrative examples

Field and laboratory measurements of thermal conductivity conducted in the scope of geothermal system design for various projects in the St. Lawrence Lowlands sedimentary basin are presented to illustrate how the reviewed methods can be implemented for regional to site-specific assessments. An overview of the St. Lawrence Lowlands geological setting is provided below to facilitate understanding the examples.

St. Lawrence Lowlands geological setting

The St. Lawrence Lowlands form a sedimentary basin covering ~20 000 km² in Southern Quebec, including major cities such as Montreal and Quebec City where geothermal systems are installed. The Cambro-Ordovician rocks of the sedimentary sequence formed in a geodynamic context evolving from a rift to a passive margin and a foreland basin (Figure 10; Globensky 1987; Comeau et al. 2013). Mineralogical phases and porosity of sedimentary groups, from clay- to quartz-rich with low to moderate porosity, are expected to affect the thermal conductivity. Water, saturated clay material and quartz have a thermal conductivity equal to 0.6, 1.5 and 7.7 W m⁻¹ K⁻¹, illustrating the thermal conductivity contrast between each phase (Clauser and Huenges 1995).

The basal sandstone of the Potsdam Group encloses the Covey Hill and Cairnside formations, constituted of 80 to 98 % quartz with an average porosity between 4 and 6 % that can locally exceed 10 % (Tran Ngoc et al. 2014). The Potsdam Group is overlain by the Beekmantown Group constituted of the Theresa and Beauharnois formations made of quartz and dolomitic sandstone evolving upward into dolostone. The Beekmantown Group has an average porosity of 1~2 % (Tran Ngoc et al. 2014). The Chazy, Black River and Trenton groups, unconformably overlying the Beauharnois Formation, are dominantly constituted of limestone and argillaceous limestone. Near the top of the Trenton Group, limestone decreases at the expense of increasing clay until the overlying Utica Shale. The Sainte-Rosalie Group, subsequently overlying the Utica Shale, comprises siltstone, mudstone, silty mudstone and occasionally dolostone showing an upward trend with decreasing clay content. The Lorraine Group, made of shale, sandstone, siltstone and limestone, overlies the Sainte-Rosalie Group, and are both turbidites. Molasses of the Queenston Group, overlying the Lorraine Group, are composed of shale with minor sandstone and siltstone, with occasional gypsum and anhydrite lenses.

Regional geothermal potential evaluation with needle probe measurements

A thermostratigraphic assessment was conducted for the Quebec portion of the St. Lawrence Lowlands to evaluate the geothermal heat pump potential of the different sedimentary rock units (Raymond et al. 2017c). A total of fifty samples were collected in surface outcrops characteristic of each sedimentary group. Holes were drilled in samples to evaluate the thermal conductivity with the needle probe method. A thermal compound was applied on the needle to ensure good contact between the needle and the samples, which were saturated when showing visible porosity. The probe used was a KD2pro model from Decagon Devices

having a heat injection rate equal to 6 W m^{-1} . The probe was initially inserted in a reference polyethylene standard and heat was injected once during a period of approximately five minutes followed by five minutes of thermal recovery to complete one analysis. The probe was then inserted in a rock sample and heat injection was repeated every hour to make at least five consecutive thermal conductivity analyses. A reference sample analysis was repeated after the series of rock sample analyses to determine a correction factor from the average of the two reference samples' analyses. The correction factor was multiplied to the rock sample analyses that are finally averaged to return the final thermal conductivity of the rock sample. This procedure was repeated for forty-five samples that remained suitable for testing after drilling the holes. The thermal conductivity was determined from the heat injection experiments with the infinite line source equation using the slope method for the heat injection (equation 14) and the recovery period (equation 20).

Evaluation of the volumetric heat capacity for each sample was necessary to find the thermal diffusivity, defined by the ratio of the thermal conductivity over the volumetric heat capacity, and perform the geothermal potential assessment with GHE sizing calculations. Thin sections of rock samples were prepared and analyzed under a petrographic microscope to estimate the main minerals and the porosity to calculate the volumetric heat capacity according to the fraction of each phase (Waples and Waples 2004a, b).

The geothermal potential was evaluated according to the rock sample thermal properties by calculating the length of GHE needed for a small-size building since GHEs are an expensive component of GCHP systems. Host rocks in which fewer GHEs can be installed for equivalent ground loads can be identified as favourable. The sizing calculations were performed with equation 1 considering the design parameters of Table 2. The borehole thermal resistance associated with the GHE was evaluated with Hellström's line-source method (1991), taking into account the subsurface thermal conductivity at the borehole wall and giving the range of values in Table 2. A similar subsurface temperature equal to $8 \text{ }^\circ\text{C}$ was assumed for all locations, which represents an average ground temperature in the upper 100 m of the sedimentary basin over the study area (Majorowicz et al. 2009).

Results from laboratory measurements were used to determine thermostratigraphic units, defined as consecutive geological layers of similar conductive heat transfer ability. Sedimentary groups or formations were combined or divided to define the thermostratigraphic units that are further constrained by their positions along the sedimentary sequence. The borehole length obtained from the sizing calculations (less than or equal to 130 m, between

130 to 160 m, or greater or equal to 160 m) was assigned a high, moderate and low geothermal potential for GCHP systems. This choice of geothermal potential associated to the borehole length is to illustrate how the subsurface thermal conductivity can affect installation costs and is relative to the SLL Lowlands since it was chosen to compare all units among each other. The geothermal potential was illustrated by a point map of thermostratigraphic units indicated by hexagons overlain by traffic light circles representing the potential, superimposed on a geological map of the area (Figure 11).

The Cairnside and Covey Hill formations of the Potsdam Group were classified in a single thermostratigraphic unit, typically having thermal conductivity above $6.0 \text{ W m}^{-1} \text{ K}^{-1}$ and showing a high geothermal potential due to the high quartz content. The overlying Theresa Formation similarly has a high thermal conductivity above $4.0 \text{ W m}^{-1} \text{ K}^{-1}$ and a high geothermal potential. The transition from sandstone of the Theresa Formation to dolostone of the Beauharnois Formation affects the thermal conductivity, decreasing toward moderate values as low as $2.7 \text{ W m}^{-1} \text{ K}^{-1}$ and justifying two distinct thermostratigraphic units for those formations. The change in mineralogy resulting in dominant limestone content with some clay for the Trenton, Black River and Chazy groups, classified as a single thermostratigraphic unit with low to moderate geothermal potential, influences the thermal conductivity ranging from 2.5 to $4.2 \text{ W m}^{-1} \text{ K}^{-1}$ and most commonly below $3.0 \text{ W m}^{-1} \text{ K}^{-1}$. The increase in clay content in the Utica Shale and the Sainte-Rosalie Group further decreases the thermal conductivity that is generally below $2.5 \text{ W m}^{-1} \text{ K}^{-1}$ in those two geological units classified as a thermostratigraphic unit with low geothermal potential. Variable lithologies in the overlying Lorraine and Queenston groups, classified as a single thermostratigraphic unit with dominantly moderate geothermal potential, show thermal conductivity values that range from 2.0 to $3.4 \text{ W m}^{-1} \text{ K}^{-1}$. It is important to note that this assessment is relative to the rock type sampled in the St. Lawrence Lowlands generally having high to moderate values when compared to the range of thermal conductivity observed for sedimentary rocks that can vary from 0.5 to $6 \text{ W m}^{-1} \text{ K}^{-1}$, although values above $4 \text{ W m}^{-1} \text{ K}^{-1}$ are less abundant (Clauser 2014b).

Subsurface thermal conductivity distribution of an urban district defined with heating cable TRT and MTPS laboratory measurements

The thermal conductivity assessment of the St. Lawrence Lowlands was studied in greater detail in a 350 km^2 region to the north of Montreal with a high population density, representing a significant market for geothermal heat pump installation (Raymond et al.

2017b). An interpolated map of the host rock thermal conductivity was produced at the urban district scale as a tool for geothermal system designers to infer thermal conductivity and facilitate GHE sizing calculations. Geostatistical simulations were performed to interpolate host rock thermal conductivity values evaluated from four TRTs with a continuous heating cable, ten laboratory measurements of outcrop samples with the modified transient plane source method and twenty-seven synthetic data points based on the above regional thermostratigraphic assessment for the simulation to reflect the local host rock distribution.

The four TRTs were performed in shallow GHEs approximately 45 m deep, which had been installed for residential geothermal heat pump systems, and the TRTs had been carried out before the GHEs were connected to the systems. The use of a continuous heating cable in shallow GHEs allowed the tests to be performed with a power source of less than 1200 W. Heat was injected for 50 to 55 h followed by the monitoring of the thermal recovery period for 60 to 72 h. Fifteen submersible temperature loggers located along the heating cable recorded data during the tests that were analyzed with the slope method for the recovery period (equation 20).

Laboratory analyses of the ten outcrop samples complementing the in situ data set were made with the MTPS method (Harris et al. 2014). Cut samples were saturated with water to apply the heat source on a flat surface heated to determine the thermal conductivity. The laboratory analyses were fast when compared to in situ assessments and yielded a greater amount of data points suitable for interpolation. The additional synthetic data points determined from the regional thermal conductivity assessment in the St. Lawrence Lowlands (Raymond et al. 2017c) were determined with random functions based on statistical thermal conductivity distribution of the thermostratigraphic units enclosed in the study area.

The distribution of host rock thermal conductivity was evaluated with sequential Gaussian simulations (Goovaerts 1997). A grid with 100×100 m cells was drawn over the study area and cells with known thermal conductivity were considered static. The Gaussian probability density function was obtained for random cells by kriging from the measured values and the previously simulated values along the random path. This feedback loop retaining previously simulated results as extra data points is to ensure that the simulations are spatially correlated. Multiple simulations were generated by using different random paths and random seeds. Independent realizations of equivalent probability were combined to calculate the mean thermal conductivity distribution and the standard deviation.

The analysis of the recovery temperature curve at a depth of 18 m for TRT 4 is given as an example, illustrating the TRT analysis process (Figure 12). The black line showing the slope of the late recovery temperature measurements illustrates that the first 10 h of recovery data were discarded to calculate the slope to find the thermal conductivity. A similar analysis of late recovery data using the slope method was repeated for the fifteen temperature sensors in each of the four GHE. The thermal conductivity evaluations obtained along each GHE were averaged to find the global thermal conductivity of the host rock over a depth of 45 m (Table 3). The example of TRT 4 shown on Figure 13 indicates a low thermal conductivity in the overburden, which was removed from analysis since the map focuses on the host rock thermal conductivity. The GHE intercepted the Trenton, Black River and Chazy geological groups, as well as the Beauharnois Formation, indicating a thermal conductivity ranging from 2.4 to 4.2 W m⁻¹ K⁻¹ (Table 3). The highest value was for the Beauharnois Formation with its greater dolomite content. The ten outcrop samples collected from the Trenton, Black River and Chazy geological groups showed a thermal conductivity ranging from 2.1 to 3.5 W m⁻¹ K⁻¹ (Table 3).

Ten independent sequential Gaussian simulations were achieved to map the thermal conductivity distribution of the host rock and were combined to define an average distribution with its standard deviation (Figure 14). The thermal conductivity distribution reflects the geological map, with values above 3.0 W m⁻¹ K⁻¹ in the upper left corner of the study area associated with the Beauharnois Formation, while values below 3.0 W m⁻¹ K⁻¹ are dominantly associated with the Trenton, Black River and Chazy groups. The map of host rock thermal conductivity can be a valuable tool to design small geothermal heat pump systems with low design risk, taking into account the probability and cost of system failure. Larger geothermal heat pump systems with significant design risk affecting GHE length require an on-site TRT to reduce the uncertainty in the subsurface thermal conductivity.

On-site conventional TRT in the Sainte-Rosalie Group

A TRT was made at INRS laboratory facilities located in Quebec City in a GHE drilled in the Sainte-Rosalie Group. The borehole installed to a depth of 154 m intercepted ~10 m of backfill material and clay, followed by shale. The objective of the test was to evaluate the borehole thermal resistance of the GHE installed with a reduced diameter of 114 mm to verify its performance (Raymond et al. 2017a). Therefore, the test included a heat injection period of 81 h as shown in Figure 15, followed by 76 h of thermal recovery monitoring with water circulation, to evaluate both the subsurface thermal conductivity and the borehole thermal

resistance. The average water flow rate in the GHE during the test was 18.9 L m^{-1} and an average power of 9693 W or 63 W/m of borehole was injected through the GHE. The flow rate and the water temperature at the inlet and outlet of the GHE were recorded every minute (Figure 15), with accuracy of 0.3% and $0.03 \text{ }^\circ\text{C}$, respectively.

The test was analyzed with the infinite line source equation using the slope method (equation 14) with heat injection data and the curve-fitting method (equation 16) with both heat injection and recovery data. The mean water temperature in the GHE was found with the p-linear average (equation 10) before proceeding with analysis. The average heat injection rate of 63 W m^{-1} determined over the entire heating period was considered for analysis with the slope method, whereas eight heat injection steps were used for the curve-fitting analysis. The heat injection steps varied from 61 to 64 W m^{-1} during the heat injection and were equal to 1 W m^{-1} during the recovery to account for the water temperature fluctuations, which can be seen on Figure 15 during the test first eighty hours.

Analysis of heat injection data with the slope method revealed a subsurface thermal conductivity equal to $2.03 \text{ W m}^{-1} \text{ K}^{-1}$. Such low thermal conductivity is in agreement with the shale rock described from the drill cuttings. Twenty-eight computed temperature points were fitted to the observed temperature during the heat injection and the recovery periods, for the curve-fitting analysis provided as an example (Figure 16). The sum of the squared residual for observed and computed temperatures was $0.69 \text{ }^\circ\text{C}^2$ and it decreased by three orders of magnitude after optimization with a non-linear solver (Lasdon et al. 1978). The analysis indicated a subsurface thermal conductivity equal to $1.75 \text{ W m}^{-1} \text{ K}^{-1}$ and a borehole thermal resistance of 0.088 m K W^{-1} . The use of variable heat injection rates allowing reproducing late heat injection and recovery temperature measurements illustrated in Figure 16 can explain the different thermal conductivity obtained with this curve-fitting method, when compared to the slope method assuming a constant heat injection rate. This borehole thermal resistance is low and indicates an improved thermal performance when compared to GHE with a diameter of 152 mm that can have a borehole thermal resistance up to $20\text{--}25 \%$ higher (Raymond et al. 2017a).

Summary

The growth of the green building industry has created opportunities to develop related services, one of which is the thermal characterization of the subsurface in the context of geothermal heat pump design. The performance of such system is affected by the thermal

state and properties of the subsurface influencing the operating temperature of closed-loop ground heat exchangers (GHEs). Ground-coupled heat pump (GCHP) systems are designed to maintain an operating temperature that will ensure sufficient energy saving under reasonable GHE length. The design of larger systems for multi-residential, institutional, commercial and industrial buildings with major energy demands involves greater operating risks that can be minimized with a proper knowledge of subsurface temperature, heat capacity and thermal conductivity. Techniques to assess the latter, which is the most critical parameter, have evolved from the Earth science sector and been adapted to GHEs.

The popular thermal response test (TRT), with heated water flowing in a GHE to infer the bulk subsurface thermal conductivity with transient heat transfer analysis, can advantageously be performed in a pilot GHE used afterward when the system is completed. Extensive research has been performed since the original TRT concept has been proposed in the 1980s (Mogensen 1983) to improve field procedures and the mathematical analysis of this active method.

Field units have been modified to incorporate a heat pump and control mechanisms to perform tests under heat extraction (Witte et al. 2002). Tests with constant temperature (Wang et al. 2010; Choi and Ooka 2017), rather than constant heat injection or extraction rate have further been introduced to reduce test time. TRTs have been coupled with distributed temperature sensing to monitor temperature at depth with optical fiber and infer the subsurface thermal conductivity along the borehole (Fujii et al. 2006, 2009, Acuña et al. 2011; Acuña and Palm 2013). This allowed the impact of subsurface heterogeneity and groundwater flow to be evaluated; for example, with the analysis of Peclet numbers (Lehr and Sass 2014). Tests with a heating element made of a cable assembly installed inside the standing water column of the GHE have further been envisioned to reduce the impact of surface temperature changes and to decrease the power requirements (Raymond et al. 2010, 2015a, Raymond and Lamarche 2014).

Analysis methods, most commonly relying on the infinite line source equation, have been improved to take into account variable heat injection rates (Beier and Smith 2003), interruptions (Beier and Smith 2005) or thermal recovery monitoring (Raymond et al. 2011b). Parameter sensitivity and stochastic estimation (Wagner and Clauser 2005; Bozzoli et al. 2011; Pasquier 2015; Choi and Ooka 2015), in addition to error calculations (Sharqawy et al. 2009; Witte 2013), have been performed to evaluate the accuracy of the TRT method. Alternative analytical or numerical models have further been proposed to improve analysis by

considering the effect of subsurface heterogeneity or groundwater flow (Signorelli et al. 2007; Raymond et al. 2011c; Wagner et al. 2013).

Passive thermal conductivity assessment methods that rely on the interpretation of a geophysical signal have also been applied to geothermal system design. The interpretation of gamma ray logs to infer the subsurface thermal conductivity was successfully achieved in boreholes drilled for GCHP systems before the installation of the pipe loop (Alonso-Sánchez et al. 2012). This example illustrates the great potential of this method where different geophysical well logs could be analyzed to find the mineralogical content and calculate the thermal conductivity with a mixing model (Brigaud et al. 1990; Dove and Williams 1990; Vasseur et al. 1995) or calculate the thermal conductivity with empirical relationships (Popov et al. 2003; Hartmann et al. 2005; Gasior and Przelaskowska 2014). A temperature profile can additionally be analyzed to infer the subsurface thermal conductivity if the Earth's heat flow is known (Rohner et al. 2005) or to extend a TRT assessment beyond a first borehole when the site basal heat flow is unknown (Raymond et al. 2016).

Field experiments conducted at the borehole scale to determine the subsurface thermal conductivity can be complemented by laboratory measurements performed at the sample scale. Active thermal conductivity assessment of an outcrop or drill core sample with heat injection experiments can be achieved in the laboratory. The steady-state divided bar method (Beck 1957), in which heat transfer is established across the whole sample, is most appropriate with solid rocks because it requires the preparation of disks with flat and parallel surfaces. Transient laboratory methods to assess the thermal conductivity, such as the needle probe (Bristow and White 1994), transient plane source (Shabbir et al. 2000) or modified transient plane source methods (Harris et al. 2014) are better suited for unconsolidated deposits or friable rocks. Such transient methods all rely on a heat pulse sent to the sample to locally disturb its thermal equilibrium and can have difficulty in providing a portrait a bulk value. Laboratory methods have been used for geothermal heat pump studies to compare results with in situ assessments in boreholes (Luo et al. 2016a) or to evaluate the spatial distribution of the subsurface thermal conductivity and establish the geothermal potential of a given region (Di Sipio et al. 2014; Galgaro et al. 2015).

Examples provided in this manuscript for the St. Lawrence Lowlands evidence the spatial limitation of the active and passive methods conducted in the field or the laboratory to assess the subsurface thermal conductivity. The radius of influence of a TRT is limited to a distance of 1 to 2 m around a borehole (Raymond et al. 2014), whereas a GHE field can cover tens to

hundreds of square metres. Passive methods additionally rely on geophysical signals having a penetration depth on the order of a few decimetres around a borehole. Thermal conductivity assessments in the laboratory are performed on centimetric samples used to assess the geothermal potential at the regional scale. Yet, the subsurface is recognized to be heterogeneous. Microscopic variations in mineralogical content, porosity and water saturation can affect the thermal conductivity of the bedrock that can change by a factor of approximately two to five within the same rock type (Clauser 2014b). Variations affecting the subsurface thermal conductivity of a given rock formation can occur at the site to the regional scale. While research has been conducted to improve thermal conductivity assessment methods, little work has been achieved to address the spatial limitation of thermal conductivity assessments. Conducting geostatistical simulations to interpolate thermal conductivity assessments (Raymond et al. 2017b) and analyzing temperature profiles to extrapolate thermal conductivity inferred in a borehole (Raymond et al. 2016) are potential solutions to the spatial limitation problem that needs to be studied in greater detail. Interpolating thermal conductivity values require scaling up punctual assessments, which were shown to be affected by the scale from the borehole to the sample (Luo et al. 2016a) and within the sample itself (Jorand et al. 2013). The spatial limitation of thermal conductivity assessment methods remains one of the main challenges to be addressed by the scientific community working on subsurface characterization to design geothermal systems.

Acknowledgements

The Banting Postdoctoral Fellowship program, the Natural Sciences and Engineering Research Council of Canada and the *Fonds de recherche du Québec – Nature et technologies* are acknowledged for funding various research projects leading to the results presented in this manuscript. The International Geoscience Program group 636 on geothermal energy, funded by UNESCO, has also supported the research performed by the author. The Canadian Geotechnical Society and the Canadian Foundation for Geotechnics are additionally acknowledged for giving the author the opportunity to present the Colloquium lecture in Vancouver in 2016, completing a Canadian lecture tour in 2017 and preparing this article. The Colloquium Lecture Series took place in Saint-Bruno-de-Montarville, Medellín (Colombia), Rouyn, Quebec City, Halifax, St. John's, Winnipeg, Edmonton, Calgary, Toronto, Reykjavik (Iceland) and Stockholm (Sweden). The Colloquium Award is a major recognition and opportunity for a starting researcher to expand his visibility for which the author is truly thankful. Final acknowledgements go to Michel Malo, Louis Lamarche, Jean-Sébastien

Gosselin and three anonymous reviewers who helped with the preparation and review of this manuscript.

References

- Acuña, J., Mogensen, P., and Palm, B. 2011. Distributed thermal response tests on a multi-pipe coaxial borehole heat exchanger. *HVAC&R Research*, **17**(6): 1012–1029. doi:10.1080/10789669.2011.625304.
- Acuña, J., and Palm, B. 2013. Distributed thermal response tests on pipe-in-pipe borehole heat exchangers. *Applied Energy*, **109**(0): 312–320. doi:10.1016/j.apenergy.2013.01.024.
- Alonso-Sánchez, T., Rey-Ronco, M.A., Carnero-Rodríguez, F.J., and Castro-García, M.P. 2012. Determining ground thermal properties using logs and thermal drill cutting analysis. First relationship with thermal response test in principality of Asturias, Spain. *Applied Thermal Engineering*, **37**(0): 226–234. doi:10.1016/j.applthermaleng.2011.11.020.
- Anderson, E.M. 1934. Earth contraction and mountain building. *Beitrage zur Geophysik*, **42**: 133–159.
- Antriasian, A., and Beardsmore, G. 2014. Longitudinal heat flow calorimetry: a method for measuring the heat capacity of rock specimens using a divided bar. *Geotechnical testing journal*, **37**(5): 858–868. doi:10.1520/GTJ20130168.
- Arato, A., Boaga, J., Comina, C., De Seta, M., Di Sipio, E., Galgaro, A., Giordano, N., and Mandrone, G. 2015. Geophysical monitoring for shallow geothermal applications - Two Italian case histories. *First Break*, **33**(8): 75–79.
- ASHRAE. 2015. Geothermal Energy. *In* ASHRAE handbook - HVAC Applications. *Edited by* ASHRAE. American Society of Heating, Refrigerating and Air-Conditioning Engineers, Atlanta. p. 34.1-34.34.
- Austin III, W.A. 1998. Development of an in situ system for measuring ground thermal properties. Master Thesis, Oklahoma State University, Oklahoma.
- Aydin, M., Onur, M., and Sisman, A. 2017. A new method for constant temperature thermal response tests. *Proceedings of the 42nd Workshop on Geothermal Reservoir Engineering*. Stanford University, Stanford, SGP-TR-212.
- Badache, M., Eslami-Nejad, P., Ouzzane, M., Aidoun, Z., and Lamarche, L. 2016. A new modeling approach for improved ground temperature profile determination. *Renewable Energy*, **85**: 436–444. doi:10.1016/j.renene.2015.06.020.

- Barry-Macaulay, D., Bouazza, A., Singh, R.M., and Wang, B. 2014. Thermal properties of some Melbourne soils and rocks. *Australian Geomechanics Journal*, **49**(2): 31–44.
- Barry-Macaulay, D., Bouazza, A., Singh, R.M., Wang, B., and Ranjith, P.G. 2013. Thermal conductivity of soils and rocks from the Melbourne (Australia) region. *Engineering Geology*, **164**: 131–138. doi:10.1016/j.enggeo.2013.06.014.
- Beck, A. 1957. A steady state method for the rapid measurement of the thermal conductivity of rocks. *Journal of Scientific Instruments*, **34**(5): 186–189. doi:10.1088/0950-7671/34/5/304.
- Beck, A.E. 1976. The use of thermal resistivity logs in stratigraphic correlation. *Geophysics*, **41**(2): 300–309.
- Beck, A.E., Anglin, F.M., and Shaw, J.H. 1971. Analysis of heat flow data - in situ thermal conductivity measurements. *Canadian Journal of Earth Sciences*, **8**: 1–19.
- Beck, A.E., and Beck, J.M. 1958. On the measurement of the thermal conductivities of rocks by observations on a divided bar apparatus. *EOS, Transactions American Geophysical Union*, **39**(6): 1111–1123. doi:10.1029/TR039i006p01111.
- Beier, R.A., Acuña, J., Mogensen, P., and Palm, B. 2012. Vertical temperature profiles and borehole resistance in a U-tube borehole heat exchanger. *Geothermics*, **44**(0): 23–32. doi:10.1016/j.geothermics.2012.06.001.
- Beier, R.A., and Smith, M.D. 2002. Borehole thermal resistance from line-source model of in-situ tests. *ASHRAE Transactions*, **108**(2): 212–219.
- Beier, R.A., and Smith, M.D. 2003. Minimum duration of in-situ tests on vertical boreholes. *ASHRAE Transactions*, **109**(3): 475–486.
- Beier, R.A., and Smith, M.D. 2005. Analyzing interrupted in-situ tests on vertical boreholes. *ASHRAE Transactions*, **111**(1): 702–713.
- Benfield, A.E. 1939. Terrestrial heat flow in Great Britain. *Proceedings of the Royal Society of London, Series A* **173**: 474–502.
- Bernier, M. 2000. A Review of the cylindrical heat source method for the design and analysis of vertical ground-coupled heat pump systems. *Proceedings of the Fourth International Conference on Heat Pumps in Cold Climates Conference*. Caneta Research Inc., Aylmer. pp. 1–14.
- Bernier, M. 2001. Ground-coupled heat pump system simulation. *ASHRAE Transactions*, **107**(1): 605–616.
- Bernier, M., Chala, A., and Pinel, P. 2008. Long-term ground-temperature changes in geo-exchange systems. *ASHRAE Transactions*, **114**(2): 342–350.

- Bozdağ, Ş., Turgut, B., Paksoy, H., Dikici, D., Mazman, M., and Evliya, H. 2008. Ground water level influence on thermal response test in Adana, Turkey. *International Journal of Energy Research*, **32**(7): 629–633. doi:10.1002/er.1378.
- Bozzoli, F., Pagliarini, G., Rainieri, S., and Schiavi, L. 2011. Estimation of soil and grout thermal properties through a TSPEP (two-step parameter estimation procedure) applied to TRT (thermal response test) data. *Energy*, **36**(2): 839–846. doi:doi: DOI: 10.1016/j.energy.2010.12.031.
- Brigaud, F., Chapman, D.S., and Le Douaran, S. 1990. Estimating thermal conductivity in sedimentary basins using lithologic data and geophysical well logs. *American Association of Petroleum Geologists Bulletin*, **74**(9): 1459–1477.
- Bristow, K.L., Kluitenberg, G.J., and Horton, R. 1994. Measurement of soil thermal properties with a dual-probe heat-pulse technique. *Soil Science Society of America Journal*, **58**(5): 1288–1294.
- Bristow, K.L., and White, R.D. 1994. Comparison of single and dual probes for measuring soil thermal properties with transient heating. *Australian Journal of Soil Research*, **32**(3): 447–464. doi:10.1071/SR9940447.
- Canadian GeoExchange Coalition. 2010. Comparative analysis of greenhouse gas emissions of various residential heating systems in the Canadian provinces. Canadian GeoExchange Coalition, Montreal.
- Canadian GeoExchange Coalition. 2012. The state of the Canadian geothermal heat pump industry 2011 - Industry survey and market analysis. Canadian GeoExchange Coalition, Montreal.
- Carslaw, H.S. 1945. *Introduction to the mathematical theory of the conduction of heat in solids*. Dover, New York.
- Chiasson, A., and O’Connell, A. 2011. New analytical solution for sizing vertical borehole ground heat exchangers in environments with significant groundwater flow: Parameter estimation from thermal response test data. *HVAC and R Research*, **17**(6): 1000–1011. doi:10.1080/10789669.2011.609926.
- Choi, W., and Ooka, R. 2015. Interpretation of disturbed data in thermal response tests using the infinite line source model and numerical parameter estimation method. *Applied Energy*, **148**: 476–488. doi:10.1016/j.apenergy.2015.03.097.
- Choi, W., and Ooka, R. 2017. Development of TPRT (thermal performance-response test) for borehole heat exchanger design. *Proceedings of IGHSPA Technical/Research*

- Conference and Expo, Denver, pp. 240–247.
doi:<http://dx.doi.org/10.22488/okstate.17.000514>.
- Claesson, J., and Hellström, G. 2011. Multipole method to calculate borehole thermal resistances in a borehole heat exchanger. *HVACR Research* 17: 859–911.
doi:[10.1080/10789669.2011.609927](http://dx.doi.org/10.1080/10789669.2011.609927)
- Clauser, C. 2014a. Thermal Storage and Transport Properties of Rocks, I: Heat Capacity and Latent Heat. *Encyclopedia of Solid Earth Geophysics*, Edited by H. Gupta, Springer Netherlands, pp. 1423–1431. doi:[10.1007/978-90-481-8702-7_238](https://doi.org/10.1007/978-90-481-8702-7_238).
- Clauser, C. 2014b. Thermal Storage and Transport Properties of Rocks, II: Thermal Conductivity and Diffusivity. *Encyclopedia of Solid Earth Geophysics*, Edited by H. Gupta, Springer Netherlands, pp. 1431–1448. doi:[10.1007/978-90-481-8702-7_67](https://doi.org/10.1007/978-90-481-8702-7_67).
- Clauser, C., and Huenges, E. 1995. Thermal conductivity of rocks and minerals. *Rock physics & phase relations; a handbook of physical constants*, AGU Reference Shelf, Edited by T.J. Ahrens. American Geophysical Union, Washington DC, USA, pp. 105–126.
- Comeau, F.-A., Bédard, K., and Malo, M. 2013. Lithostratigraphie standardisée du bassin des Basses-Terres du Saint-Laurent basée sur l'étude des diagraphies. Report R1442, Institut national de la recherche scientifique, Quebec City.
- Cooper, H.H., and Jacob, C.E. 1946. A generalized graphical method for evaluating formation constants and summarizing well field history. *American Geophysical Union Transactions*, **27**(4): 526–534.
- Côté, J., Grosjean, V., and Konrad, J.-M. 2013. Thermal conductivity of bitumen concrete. *Canadian Journal of Civil Engineering*, **40**(2): 172–180. doi:[10.1139/cjce-2012-0159](https://doi.org/10.1139/cjce-2012-0159).
- Côté, J., and Konrad, J.-M. 2005. Thermal conductivity of base-course materials. *Canadian Geotechnical Journal*, **42**(1): 61–78. doi:[10.1139/t04-081](https://doi.org/10.1139/t04-081).
- Dehkordi, S.E., and Schincariol, R.A. 2014. Effect of thermal-hydrogeological and borehole heat exchanger properties on performance and impact of vertical closed-loop geothermal heat pump systems. *Hydrogeol. J.*, **22**:189–203. doi:[10.1007/s10040-013-1060-6](https://doi.org/10.1007/s10040-013-1060-6)
- Demongodin, L., Pinoteau, B., Vasseur, G., and Gable, R. 1991. Thermal conductivity and well logs: a case study in the Paris basin. *Geophysical Journal International*, **105**(3): 675–691. doi:[10.1111/j.1365-246X.1991.tb00805.x](https://doi.org/10.1111/j.1365-246X.1991.tb00805.x).
- Di Sipio, E., Galgaro, A., Destro, E., Teza, G., Chiesa, S., Giaretta, A., and Manzella, A. 2014. Subsurface thermal conductivity assessment in Calabria (southern Italy): a

- regional case study. *Environmental Earth Sciences*, **72**: 1383–1401.
doi:10.1007/s12665-014-3277-7.
- Dove, R.E., and Williams, C.F. 1990. Thermal conductivity estimated from elemental concentration logs. *Nuclear Geophysics*, **3**(2): 107–112.
- Eskilson, P. 1987. Thermal analysis of heat extraction boreholes. Lund Institute of Technology, Department of mathematical physics, Lund.
- Ferguson, G., and Woodbury, A.D. 2004. Subsurface heat flow in an urban environment. *Journal of Geophysical Research B: Solid Earth*, **109**(2): B02402 1-9.
- Ferguson, G. 2015. Screening for heat transport by groundwater in closed geothermal systems. *Groundwater*, **53**: 503–506. doi:10.1111/gwat.12162
- Florides, G., and Kalogirou, S. 2007. Ground heat exchangers - A review of systems, models and applications. *Renewable Energy*, **32**(15): 2461–2478.
doi:10.1016/j.renene.2006.12.014.
- Fourier, J.B.J. 1822. *Théorie analytique de la chaleur*. F. Didot, Paris.
- Fuchs, S., and Förster, A. 2013. Well-log based prediction of thermal conductivity of sedimentary successions: A case study from the north german basin. *Geophysical Journal International*, **196**(1): 291–311. doi:10.1093/gji/ggt382.
- Fujii, H., Okubo, H., and Itoi, R. 2006. Thermal response tests using optical fiber thermometers. *GRC transactions*, **30**: 545–551.
- Fujii, H., Okubo, H., Nishi, K., Itoi, R., Ohyama, K., and Shibata, K. 2009. An improved thermal response test for U-tube ground heat exchanger based on optical fiber thermometers. *Geothermics*, **38**(4): 399–406. doi:10.1016/j.geothermics.2009.06.002.
- Galgaro, A., Di Sipio, E., Teza, G., Destro, E., De Carli, M., Chiesa, S., Zarrella, A., Emmi, G., and Manzella, A. 2015. Empirical modeling of maps of geo-exchange potential for shallow geothermal energy at regional scale. *Geothermics*, **57**: 173–184.
doi:10.1016/j.geothermics.2015.06.017.
- Gasior, I., and Przelaskowska, A. 2014. Estimating thermal conductivity from core and well log data. *Acta Geophysica*, **62**(4): 785–801. doi:10.2478/s11600-014-0204-y.
- Gegenhuber, N., and Schoen, J. 2012. New approaches for the relationship between compressional wave velocity and thermal conductivity. *Journal of Applied Geophysics*, **76**: 50–55. doi:10.1016/j.jappgeo.2011.10.005.
- Gehlin, S. 1998. Thermal response test - in-situ measurements of thermal properties in hard rock. Licentiate Thesis, Luleå University of Technology, Division of Water Resources Engineering, Department of Environmental Engineering, Luleå.

- Gehlin, S., and Nordell, B. 2003. Determining undisturbed ground temperature for thermal response test. *ASHRAE Transactions*, **109**: 151–156.
- Giordano, N., Comina, C., and Mandrone, G. 2016. Laboratory scale geophysical measurements aimed at monitoring the thermal affected zone in Underground Thermal Energy Storage (UTES) applications. *Geothermics*, **61**: 121–134.
doi:10.1016/j.geothermics.2016.01.011.
- Globensky, Y. 1987. *Géologie des Basses-Terres du Saint-Laurent*. Ministère de l'Énergie et des Ressources du Québec, Quebec City.
- Goovaerts, P. 1997. *Geostatistics for Natural Resources Evaluation*. Oxford University Press, New York.
- Goutorbe, B., Lucazeau, F., and Bonneville, A. 2007. Comparaison of several BHT correction methods: a case study on an Australian data set. *Geophysical Journal International*, **170**(2): 913–922.
- Grasby, S.E., Allen, D.M., Chen, Z., Ferguson, G., Jessop, A.M., Kelman, M., Ko, M., Majorowicz, J., Moore, M., Raymond, J., and Therrien, R. 2011. Geothermal energy resource potential of Canada. Open file 6914, Geological Survey of Canada, Calgary.
- Hackel, S., Nellis, G., and Klein, S. 2009. Optimization of cooling-dominated hybrid ground-coupled heat pump systems. *ASHRAE Transactions*, **115**(1): 565–580.
- Hackel, S., and Pertzborn, A. 2011. Building on experience with hybrid ground source heat pump systems. *ASHRAE Transactions*, **117**(2): 271–278.
- Harris, A., Kazachenko, S., Bateman, R., Nickerson, J., and Emanuel, M. 2014. Measuring the thermal conductivity of heat transfer fluids via the modified transient plane source (MTPS). *Journal of Thermal Analysis and Calorimetry*, **116**(3): 1309–1314.
doi:10.1007/s10973-014-3811-6.
- Hartmann, A., Rath, V., and Clauser, C. 2005. Thermal conductivity from core and well log data. *International Journal of Rock Mechanics and Mining Sciences*, **42**(7–8 SPEC. ISS.): 1042–1055. doi:10.1016/j.ijrmms.2005.05.015.
- Hellström, G. 1991. Ground heat storage; thermal analysis of duct storage systems. Ph.D. Thesis, Department of mathematical physics, University of Lund, Lund.
- Holmberg, H., Acuña, J., Næss, E., and Sønju, O.K. 2016. Thermal evaluation of coaxial deep borehole heat exchangers. *Renewable Energy*, **97**: 65–76.
doi:10.1016/j.renene.2016.05.048.

- Horton, R., Wierenga, P.J., and Nielsen, D.R. 1983. Evaluation of methods for determining the apparent thermal diffusivity of soil near the surface. *Soil Science Society of America Journal* **47**(1): 25–32.
- Ingersoll, L.R., Zobel, O.J., and Ingersoll, A.C. 1954. *Heat conduction, with engineering, geological, and other applications*. McGraw-Hill, New York.
- Jorand, R., Vogt, C., Marquart, G., and Clauser, C. 2013. Effective thermal conductivity of heterogeneous rocks from laboratory experiments and numerical modeling. *Journal of Geophysical Research: Solid Earth*, **118**(10): 5225–5235.
- Kavanaugh, S.P. 2001. Investigation of methods for determining soil formation thermal characteristics from short term field tests. American Society of Heating, Refrigerating and Air-Conditioning Engineers, Atlanta.
- Kavanaugh, S.P., and Rafferty, K. 2014. *Ground-source heat pumps: design of geothermal systems for commercial and institutional buildings*. American Society of Heating, Refrigerating and Air-Conditioning Engineers, Atlanta.
- Kohl, T. 1998. Palaeoclimatic temperature signals — can they be washed out? *Heat Flow and the Structure of the Lithosphere - IV*, **291**(1–4): 225–234. doi:10.1016/S0040-1951(98)00042-0.
- Kohl, T. 1999. Transient thermal effects below complex topographies. *Tectonophysics*, **306**(3–4): 311–324.
- Kukkonen, I.T., and Peltoniemi, S. 1998. Relationships between thermal and other petrophysical properties of rocks in Finland. *Physics and Chemistry of the Earth*, **23**(3): 341–349. doi:10.1016/S0079-1946(98)00035-4.
- Lamarche, L., Kajl, S., and Beauchamp, B. 2010. A review of methods to evaluate borehole thermal resistances in geothermal heat-pump systems. *Geothermics*, **39**(2): 187–200. doi:10.1016/j.geothermics.2010.03.003.
- Lasdon, L.S., Waren, A.D., Jain, A., and Ratner, M. 1978. Design and testing of a generalized reduced gradient code for nonlinear programming. *ACM Transactions on Mathematical Software*, **4**(1): 34–49.
- Lehr, C., and Sass, I. 2014. Thermo-optical parameter acquisition and characterization of geologic properties: a 400-m deep BHE in a karstic alpine marble aquifer. *Environmental Earth Sciences*, **72**: 1403-1419. doi:10.1007/s12665-014-3310-x.
- Lister, C.R.B. 1979. The pulse-probe method of conductivity measurement. *Geophys. J. Int.* **57**(2): 451–461. doi.org/10.1111/j.1365-246X.1979.tb04788.x

- Liu, Y.D., and Beier, R.A. 2009. Required duration for borehole test validated by field data. *ASHRAE Transactions*, **115**(2): 782–792.
- Luo, J., Jia, J., Zhao, H., Zhu, Y., Guo, Q., Cheng, C., Tan, L., Xiang, W., Rohn, J., and Blum, P. 2016a. Determination of the thermal conductivity of sandstones from laboratory to field scale. *Environmental Earth Sciences*, **75**(16): 1158. doi:10.1007/s12665-016-5939-0.
- Luo, J., Rohn, J., Xiang, W., Bertermann, D., and Blum, P. 2016b. A review of ground investigations for ground source heat pump (GSHP) systems. *Energy and Buildings*, **117**: 160–175. doi:10.1016/j.enbuild.2016.02.038.
- Majorowicz, J.A., Grasby, S.E., and Skinner, W.C. 2009. Estimation of shallow geothermal energy resource in Canada: heat gain and heat sink. *Natural Resources Research*, **18**(2): 95–108. doi:10.1007/s11053-009-9090-4.
- Marcotte, D., and Pasquier, P. 2008. On the estimation of thermal resistance in borehole thermal conductivity test. *Renewable Energy*, **33**(11): 2407–2415.
- Martos, J., Montero, Á., Torres, J., Soret, J., Martínez, G., and García-Olcina, R. 2011. Novel wireless sensor system for dynamic characterization of borehole heat exchangers. *Sensors*, **11**(7): 7082–7094. doi:10.3390/s110707082.
- Midttømme, K., Roaldset, E., and Aagaard, P. 1998. Thermal conductivity of selected claystones and mudstones from England. *Clay Minerals*, **33**(1): 131–145.
- Mogensen, P. 1983. Fluid to duct wall heat transfer in duct system heat storages. *International Conference on Subsurface Heat Storage in Theory and Practice*, Stockholm, pp. 652–657.
- Molina-Giraldo, N., Blum, P., Zhu, K., Bayer, P., and Fang, Z. 2011. A moving finite line source model to simulate borehole heat exchangers with groundwater advection. *International Journal of Thermal Science* **50**(12): 2506–2513. doi.org/10.1016/j.ijthermalsci.2011.06.012
- Nasr, M. 2016. Évaluation des propriétés thermiques de la Plate-forme du Saint-Laurent : Mesures au laboratoire et approche diagraphique. Master Thesis, Institut national de la recherche scientifique, Quebec City.
- Neville, C.J., and van der Kamp, G. 2012. Using recovery data to extend the effective duration of pumping tests. *Ground Water*, **50**: 804–807. doi:10.1111/j.1745-6584.2011.00906.x
- Omer, A.M. 2008. Ground-source heat pumps systems and applications. *Renewable & Sustainable Energy Reviews*, **12**(2): 344–371. doi:10.1016/j.rser.2006.10.003.

- Pasquier, P. 2015. Stochastic interpretation of thermal response test with TRT-SInterp. *Computers and Geosciences*, **75**: 73–87. doi:10.1016/j.cageo.2014.11.001.
- Pehme, P.E., Greenhouse, J.P., and Parker, B.L. 2007. The active line source temperature logging technique and its application in fractured rock hydrogeology. *Journal of Environmental and Engineering Geophysics*, **12**(4): 307–322. doi:10.2113/jeeeg12.4.307.
- Philippe, M., Bernier, M., and Marchio, D. 2009. Validity ranges of three analytical solutions to heat transfer in the vicinity of single boreholes. *Geothermics*, **38**(4): 407–413. doi:10.1016/j.geothermics.2009.07.002.
- Philippe, M., Bernier, M., and Marchio, D. 2010. Sizing calculation spreadsheet - Vertical geothermal borefields. *ASHRAE Journal*, **52**(7): 20–28.
- Popov, Y., Tertychnyi, V., Romushkevich, R., Korobkov, D., and Pohl, J. 2003. Interrelations between thermal conductivity and other physical properties of rocks: Experimental data. *Pure and Applied Geophysics*, **160**(5–6): 1137–1161.
- Pribnow, D., Williams, C.F., and Burkhardt, H. 1993. Well log-derived estimates of thermal conductivity in crystalline rocks penetrated by the 4-KM deep KTB Vorbohrung. *Geophysical Research Letters*, **20**(12): 1155–1158. doi:10.1029/93GL00480.
- Radioti, G., Delvoie, S., Charlier, R., Dumont, G., and Nguyen, F. 2016. Heterogeneous bedrock investigation for a closed-loop geothermal system: A case study. *Geothermics*, **62**: 79–92. doi:10.1016/j.geothermics.2016.03.001.
- Rainieri, S., Bozzoli, F., and Pagliarini, G. 2011. Modeling approaches applied to the thermal response test: A critical review of the literature. *HVAC&R Research*, **17**(6): 977–990. doi:10.1080/10789669.2011.610282.
- Raymond, J., Ballard, J.-M., and Koubikana Pambou, C.H. 2017a. Field assessment of a ground heat exchanger performance with a reduced borehole diameter. *Proceedings of the 70th Canadian Geotechnical Conference and the 12th Joint CGS/IAH-CNC Groundwater Conference*, Ottawa.
- Raymond, J., and Lamarche, L. 2013. Simulation of thermal response tests in a layered subsurface. *Applied Energy*, **109**(0): 293–301. doi:10.1016/j.apenergy.2013.01.033.
- Raymond, J., and Lamarche, L. 2014. Development and numerical validation of a novel thermal response test with a low power source. *Geothermics*, **51**: 434–444. doi:10.1016/j.geothermics.2014.02.004.
- Raymond, J., Lamarche, L., and Blais, M.-A. 2014. Quality control assessment of vertical ground heat exchangers. *ASHRAE Transactions*, **120**(2): SE-14-014.

- Raymond, J., Lamarche, L., and Malo, M. 2015a. Field demonstration of a first thermal response test with a low power source. *Applied Energy*, **147**: 30–39. doi:10.1016/j.apenergy.2015.01.117.
- Raymond, J., Lamarche, L., and Malo, M. 2016. Extending thermal response test assessments with inverse numerical modeling of temperature profiles measured in ground heat exchangers. *Renewable Energy*, **99**: 614–621. doi:10.1016/j.renene.2016.07.005.
- Raymond, J., Malo, M., Lamarche, L., Perozzi, L., Gloaguen, E., and Bégin, C. 2017b. New methods to spatially extend thermal response test assessments. Proceedings of IGHSPA Technical/Research Conference and Expo, Denver, pp. 256–265. doi:http://dx.doi.org/10.22488/okstate.17.000519.
- Raymond, J., Mercier, S., and Nguyen, L. 2015b. Designing coaxial ground heat exchangers with a thermally enhanced outer pipe. *Geothermal Energy*, **3**(7): 14. doi:10.1186/s40517-015-0027-3.
- Raymond, J., Robert, G., Therrien, R., and Gosselin, L. 2010. A novel thermal response test using heating cables. Proceedings of the World Geothermal Congress, Bali, Indonesia. pp. 1–8.
- Raymond, J., Sirois, C., Nasr, M., and Malo, M. 2017c. Evaluating the geothermal heat pump potential from a thermostratigraphic assessment of rock samples in the St. Lawrence Lowlands, Canada. *Environmental Earth Sciences*, **76**(2): 83. doi:10.1007/s12665-017-6398-y.
- Raymond, J., Therrien, R., and Gosselin, L. 2011a. Borehole temperature evolution during thermal response tests. *Geothermics*, **40**(1): 69–78. doi:10.1016/j.geothermics.2010.12.002.
- Raymond, J., Therrien, R., Gosselin, L., and Lefebvre, R. 2011b. A review of thermal response test analysis using pumping test concepts. *Ground Water*, **49**(6): 932–945. doi:10.1111/j.1745-6584.2010.00791x.
- Raymond, J., Therrien, R., Gosselin, L., and Lefebvre, R. 2011c. Numerical analysis of thermal response tests with a groundwater flow and heat transfer model. *Renewable Energy*, **36**(1): 315–324. doi:10.1016/j.renene.2010.06.044.
- Remund, C.P. 1999. Borehole thermal resistance: Laboratory and field studies. *ASHRAE Transactions* 105: 439–445.
- Rohner, E., Rybach, L., and Schärli, U. 2005. A new, small, wireless instrument to determine ground thermal conductivity in-situ for borehole heat exchanger design. Proceedings of the World Geothermal Congress, Antalya, pp. 1–4.

- Rolando, D., Acuña, J., and Fossa, M. 2017. Heat extraction distributed thermal response test: A methodological approach and in-situ experiment. Proceedings of IGHSPA Technical/Research Conference and Expo, Denver, pp. 296–304.
doi:<http://dx.doi.org/10.22488/okstate.17.000536>.
- Rouleau, J., Gosselin, L., and Raymond, J. 2016. New concept of combined hydro-thermal response tests (H/TRTS) for ground heat exchangers. *Geothermics*, **62**: 103–114.
doi:[10.1016/j.geothermics.2016.03.002](https://doi.org/10.1016/j.geothermics.2016.03.002).
- Sanner, B., Hellstrom, G., Spitler, J.D., and Gehlin, S. 2005. Thermal response test - Current status and world-wide application. Proceedings of the World Geothermal Congress. Antalya.
- Shabbir, G., Maqsood, A., and Majid, C.A. 2000. Thermophysical properties of consolidated porous rocks. *Journal of Physics D: Applied Physics*, **33**(6): 658–661.
doi:[10.1088/0022-3727/33/6/311](https://doi.org/10.1088/0022-3727/33/6/311).
- Sharqawy, M.H., Mokheimer, E.M., Habib, M.A., Badr, H.M., Said, S.A., and Al-Shayea, N.A. 2009. Energy, exergy and uncertainty analyses of the thermal response test for a ground heat exchanger. *International Journal of Energy Research*, **33**(6): 582–592.
- Signorelli, S., Bassetti, S., Pahud, D., and Kohl, T. 2007. Numerical evaluation of thermal response tests. *Geothermics*, **36**(2): 141–166. doi:[10.1016/j.geothermics.2006.10.006](https://doi.org/10.1016/j.geothermics.2006.10.006).
- Signorelli, S., and Kohl, T. 2004. Regional ground surface temperature mapping from meteorological data. *Global and Planetary Change*, **40**(3–4): 267–284.
doi:[10.1016/j.gloplacha.2003.08.003](https://doi.org/10.1016/j.gloplacha.2003.08.003).
- Siska, P., Latal, J., Bujok, P., Vanderka, A., Klempa, M., Koudelka, P., Vasinek, V., and Pospisil, P. 2016. Optical fiber based distributed temperature systems deployment for measurement of boreholes temperature profiles in the rock massif. *Optical and Quantum Electronics*, **48**(2): 1–21. doi:[10.1007/s11082-016-0379-3](https://doi.org/10.1007/s11082-016-0379-3).
- Spitler, J.D., and Gehlin, S.E.A. 2015. Thermal response testing for ground source heat pump systems—An historical review. *Renewable and Sustainable Energy Reviews*, **50**: 1125–1137. doi:[10.1016/j.rser.2015.05.061](https://doi.org/10.1016/j.rser.2015.05.061).
- Sundberg, J., Back, P.-E., Ericsson, L.O., and Wrafter, J. 2009. Estimation of thermal conductivity and its spatial variability in igneous rocks from in situ density logging. *International Journal of Rock Mechanics and Mining Sciences*, **46**(6): 1023–1028.
doi:[10.1016/j.ijrmms.2009.01.010](https://doi.org/10.1016/j.ijrmms.2009.01.010).

- Theis, C.V. 1935. The relation between the lowering of the piezometric surface and the rate and duration of a well using groundwater storage. *American Geophysical Union Transactions*, **16**(2): 519–524.
- Tran Ngoc, T.D., Lefebvre, R., Konstantinovskaya, E., and Malo, M. 2014. Characterization of deep saline aquifers in the Bécancour area, St. Lawrence Lowlands, Québec, Canada: Implications for CO₂ geological storage. *Environmental Earth Sciences*, **72**(1): 119–146. doi:10.1007/s12665-013-2941-7.
- Vacquier, V. 1985. The measurement of thermal conductivity of solids with a transient linear heat source on the plane surface of a poorly conducting body. *Earth and Planetary Science Letters*, **74**(2–3): 275–279. doi:10.1016/0012-821X(85)90027-5.
- Vasseur, G., Brigaud, F., and Demongodin, L. 1995. Thermal conductivity estimation in sedimentary basins. *Tectonophysics*, **244**(1–3): 167–174. doi:10.1016/0040-1951(94)00225-X.
- Wagner, R., and Clauser, C. 2005. Evaluating thermal response tests using parameter estimation for thermal conductivity and thermal capacity. *Journal of Geophysics and Engineering*, **2**(4): 349–356.
- Wagner, V., Blum, P., Kübert, M., and Bayer, P. 2013. Analytical approach to groundwater-influenced thermal response tests of grouted borehole heat exchangers. *Geothermics*, **46**: 22–31. doi:10.1016/j.geothermics.2012.10.005.
- Wang, H., Qi, C., Du, H., and Gu, J. 2010. Improved method and case study of thermal response test for borehole heat exchangers of ground source heat pump system. *Renewable Energy*, **35**(3): 727–733. doi:10.1016/j.renene.2009.08.013.
- Waples, D.W., and Waples, J.S. 2004a. A review and evaluation of specific heat capacities of rocks, minerals, and subsurface fluids. Part 1: minerals and nonporous rocks. *Natural Resources Research*, **13**(2): 97–122. doi:10.1023/B:NARR.0000032647.41046.e7.
- Waples, D.W., and Waples, J.S. 2004b. A review and evaluation of specific heat capacities of rocks, minerals, and subsurface fluids. Part 2: fluids and porous rocks. *Natural Resources Research*, **13**(2): 123–130. doi:10.1023/B:NARR.0000032648.15016.49.
- Williams, G.P., and Gold, L.W. 1976. Ground temperatures. *Canadian Building Digest* 180.
- Witte, H.J.L. 2013. Error analysis of thermal response tests. *Applied Energy*, **109**(0): 302–311. doi:10.1016/j.apenergy.2012.11.060.
- Witte, H.J.L., van Gelder, G., and Spitler, J.D. 2002. In-situ thermal conductivity testing: A dutch perspective. *ASHRAE Transactions*, **108**(1): 263–272.

- Yu, X., Zhang, Y., Deng, N., Ma, H., and Dong, S. 2016. Thermal response test for ground source heat pump based on constant temperature and heat-flux methods. *Applied Thermal Engineering*, **93**: 678–682. doi:10.1016/j.applthermaleng.2015.10.007.
- Zhang, C., Guo, Z., Liu, Y., Cong, X., and Peng, D. 2014. A review on thermal response test of ground-coupled heat pump systems. *Renewable and Sustainable Energy Reviews*, **40**: 851–867. doi:10.1016/j.rser.2014.08.018.
- Zhu, K., Blum, P., Ferguson, G., Balke, K.-D., and Bayer, P. 2010. The geothermal potential of urban heat islands. *Environmental Research Letters*, **5**(4): 6 pp.

Nomenclature

b (K)	Intercept of temperature vs logarithmic time graph for heat injection test
c (J kg ⁻¹ K ⁻¹)	Specific heat capacity
Fo (-)	Fourier number
G (-)	Thermal response function
GR (API)	Gamma ray in America Petroleum Institute unit
H (m)	Thickness
L (m)	Length
m (K s ⁻¹)	Slope of temperature vs logarithmic time graph for heat injection test
\tilde{m} (K s ⁻¹)	Slope of temperature vs logarithmic time graph for recovery test
n (-)	Fraction of component
P (W)	Power
p (-)	Fitting parameter
Q (W)	Heat transfer rate
Q' (m ³ s ⁻¹)	Volumetric flow rate
q (W m ⁻¹)	Heat transfer rate per unit length
q^* (W m ⁻²)	Heat transfer rate per unit area
R (m K W ⁻¹)	Thermal resistance
r (m)	Radius
\tilde{r} (-)	Nondimensional radius
T (K)	Temperature
\bar{T} (K)	Average temperature
t (s)	Time
\tilde{t} (-)	Nondimensional time

Greek symbols and operators

Π	Product of terms
-------	------------------

Σ	Summation of terms
Δ	Increment or derivative
α ($\text{m}^2 \text{s}^{-1}$)	Thermal diffusivity
γ (0.5772...)	Euler constant
θ (-)	Neutron porosity
λ ($\text{W m}^{-1} \text{K}^{-1}$)	Thermal conductivity
ρ (kg m^3)	Density

Subscripts

ari	Arithmetic
b	Borehole
geo	Geometric
h	Hour
har	Harmonic
ICS	Infinite cylindrical source
ILS	Infinite line source
i	In, inlet, step or component of summation
m	Month
max	Maximum
min	Minimum
N	Last step or component of summation
o	Out, outlet
off	End of heat injection
p	p-average
pen	penalty
ref	Reference
s	Subsurface

ss	Sandstone
w	Water
yr	Year
0	Initial condition

Figure Captions

Figure 1. Ground-coupled heat pump system in heating mode.

Figure 2. Capacity (CAP) and coefficient of performance (COP) of a water-to-air heat pump system in heating and cooling mode according to the temperature and flow rate of the water entering the system. The COP is defined as $COP_{\text{heating}} = (Q_{\text{ground}} + P_{\text{compressor}})/P_{\text{compressor}}$ in heating mode and $COP_{\text{cooling}} = (Q_{\text{ground}} - P_{\text{compressor}})/P_{\text{compressor}}$ in cooling mode.

Figure 3. Conventional thermal response test unit (Raymond et al. 2011b).

Figure 4. Numerical simulation of temperature and heat injection rate along the pipe of a ground heat exchanger for nine days of heat extraction simulation at a constant rate equals to 7500 W (Redrawn from Marcotte and Pasquier 2008).

Figure 5. Numerical simulation of the temperature distribution in a slice of ground heat exchanger for a thermal response test with 50 h of heat injection (Raymond et al. 2011a). The borehole, having a diameter equal to 0.15 m, and the pipe circumferences are shown with continuous and dashed circles.

Figure 6. Thermal response test with a heating cable (Raymond and Lamarche 2014).

Figure 7. Approaches for well log analysis to infer the subsurface thermal conductivity (Nasr 2016). Gamma ray; GR , Density; D , Neutron porosity; θ , Photoelectric factor; PF , Transit time; TT .

Figure 8. Divided bar to measure steady-state or bulk thermal conductivity of rock samples.

Figure 9. Transient methods to measure thermal conductivity of rock samples.

Figure 10. Stratigraphic columns showing the St. Lawrence Lowlands sedimentary sequence (Comeau et al. 2013).

Figure 11. Geothermal heat pump potential of thermostratigraphic units in the St. Lawrence Lowlands (Raymond et al. 2017c).

Figure 12. Thermal conductivity analysis at a depth of 18 m for TRT 4 (Table 3), conducted with a continuous heating cable in the Beauharnois Formation.

Figure 13. Thermal conductivity profile determined for TRT 4 (Table 3) conducted with a continuous heating cable in the Beauharnois Formation.

Figure 14. Sequential Gaussian simulations to map the thermal conductivity distribution in an urban district of Montreal (Raymond et al. 2017b).

Figure 15. Water temperature and heat injection rate recorded during the conventional TRT at INRS laboratory for a borehole drilled in the Sainte-Rosalie Group.

Figure 16. Curve-fitting analysis of conventional TRT at INRS laboratory for a borehole drilled in the Sainte-Rosalie Group.

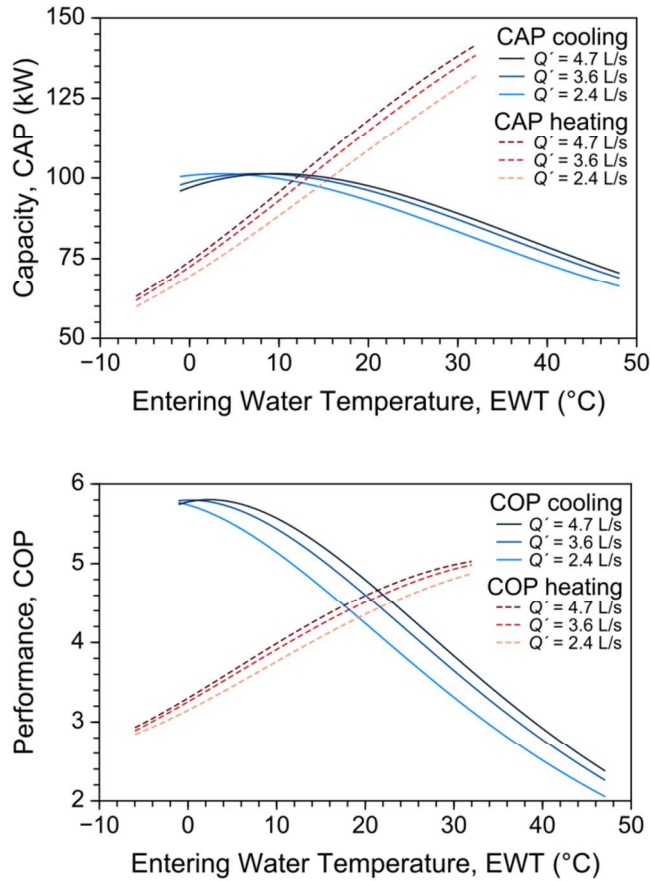


Figure 2. Capacity (CAP) and coefficient of performance (COP) of a water-to-air heat pump system in heating and cooling mode according to the temperature and flow rate of the water entering the system. The COP is defined as $COP_{\text{heating}} = (Q_{\text{ground}} + P_{\text{compressor}})/P_{\text{compressor}}$ in heating mode and $COP_{\text{cooling}} = (Q_{\text{ground}} - P_{\text{compressor}})/P_{\text{compressor}}$ in cooling mode.

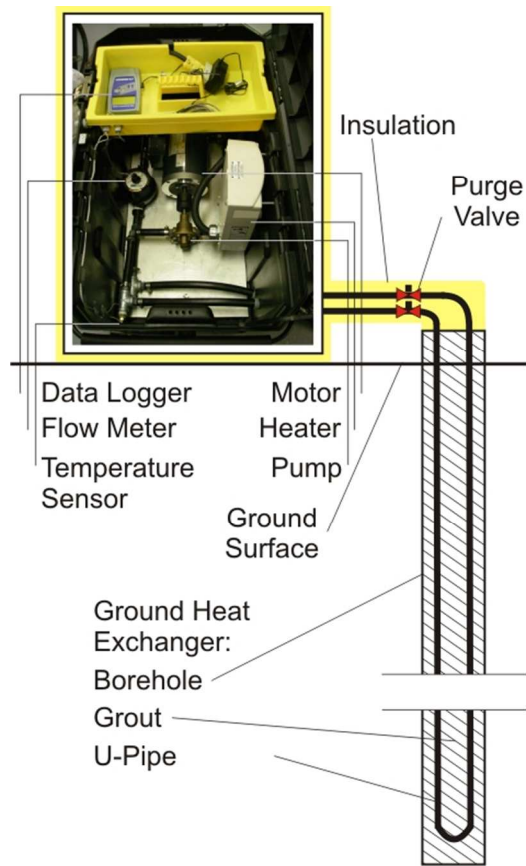


Figure 3. Conventional thermal response test unit (Raymond et al. 2011b).

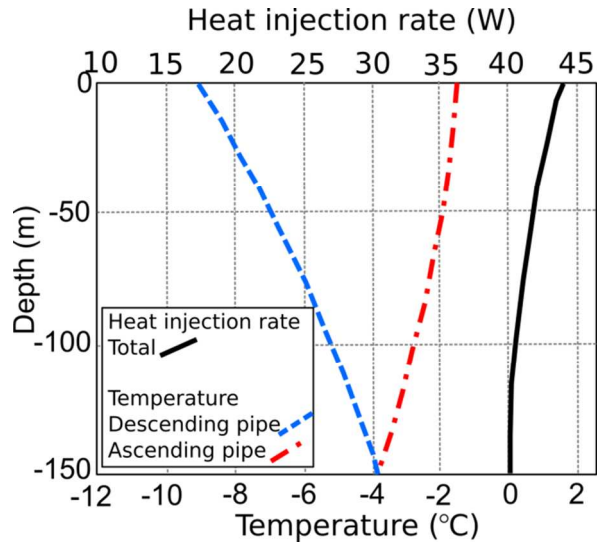


Figure 4. Numerical simulation of temperature and heat injection rate along the pipe of a ground heat exchanger for nine days of heat extraction simulation at a constant rate equals to 7500 W (Redrawn from Marcotte and Pasquier 2008).

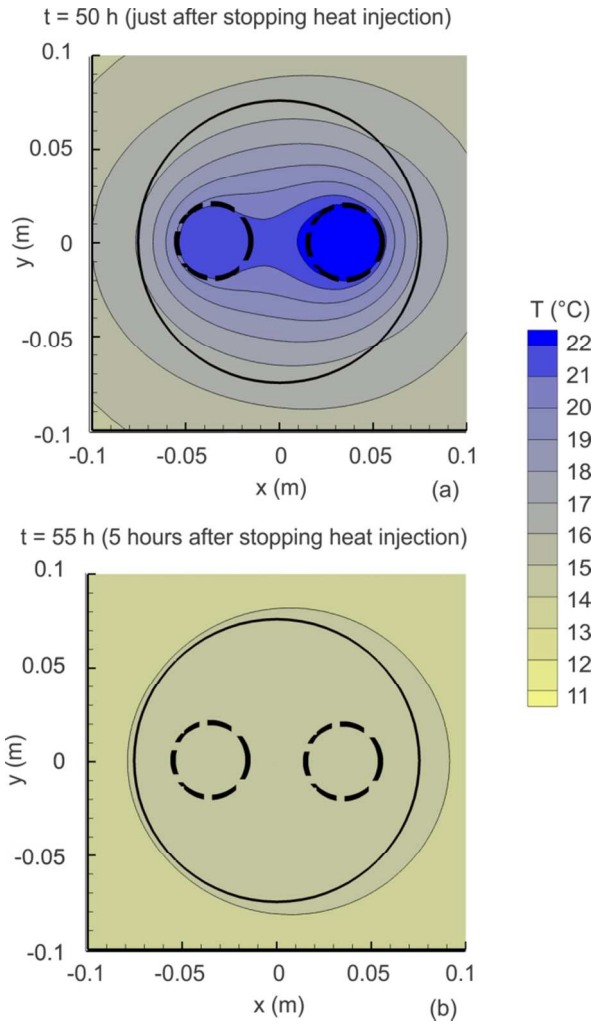


Figure 5. Numerical simulation of the temperature distribution in a slice of ground heat exchanger for a thermal response test with 50 h of heat injection (Raymond et al. 2011a). The borehole, having a diameter equal to 0.15 m, and the pipe circumferences are shown with continuous and dashed circles.

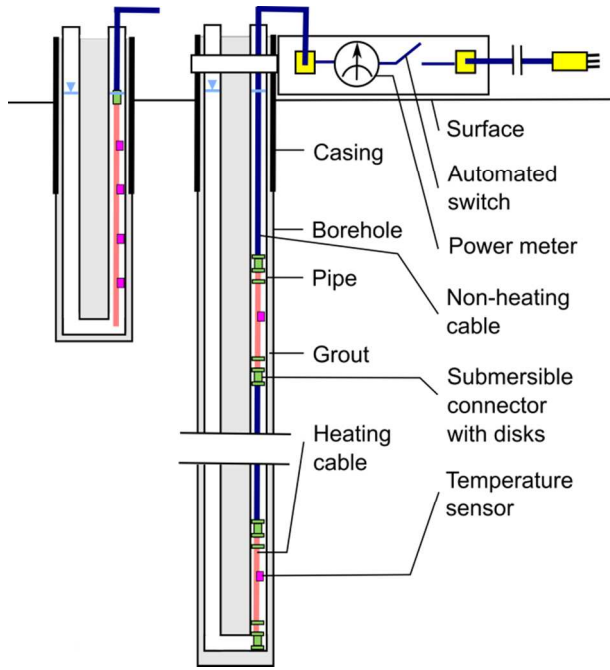


Figure 6. Thermal response test with a heating cable (Raymond and Lamarche 2014).

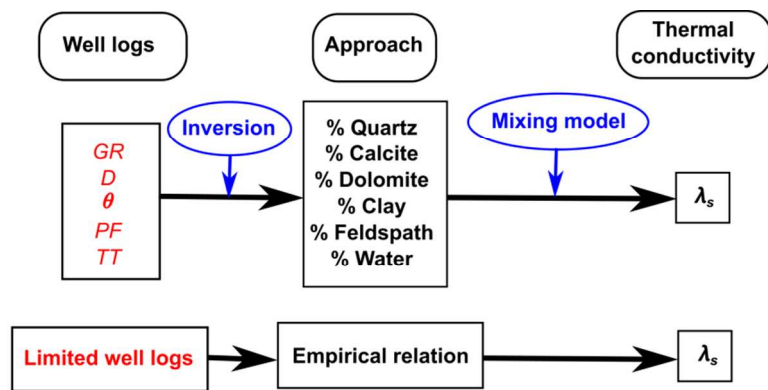


Figure 7. Approaches for well log analysis to infer the subsurface thermal conductivity (Nasr 2016). Gamma ray; GR , Density; D , Neutron porosity; θ , Photoelectric factor; PF , Transit time; TT .

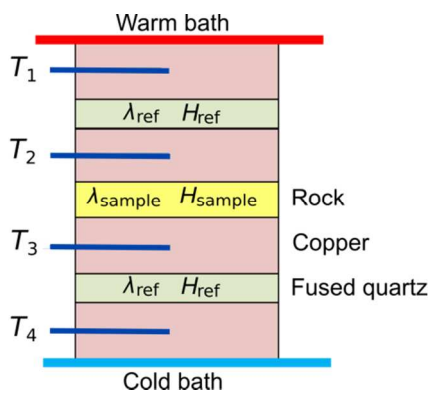


Figure 8. Divided bar to measure steady-state or bulk thermal conductivity of rock samples.

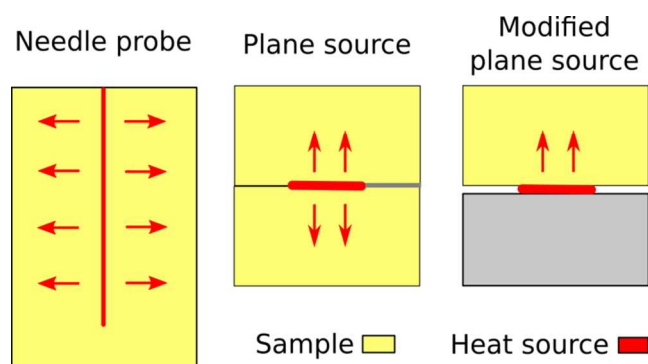


Figure 9. Transient methods to measure thermal conductivity of rock samples.

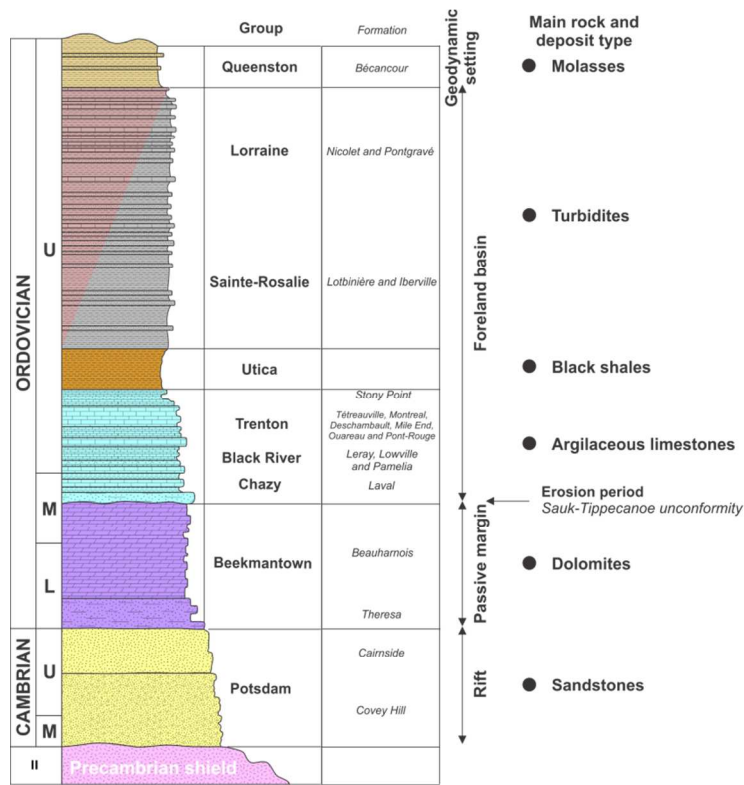


Figure 10. Stratigraphic columns showing the St. Lawrence Lowlands sedimentary sequence (Comeau et al. 2013).

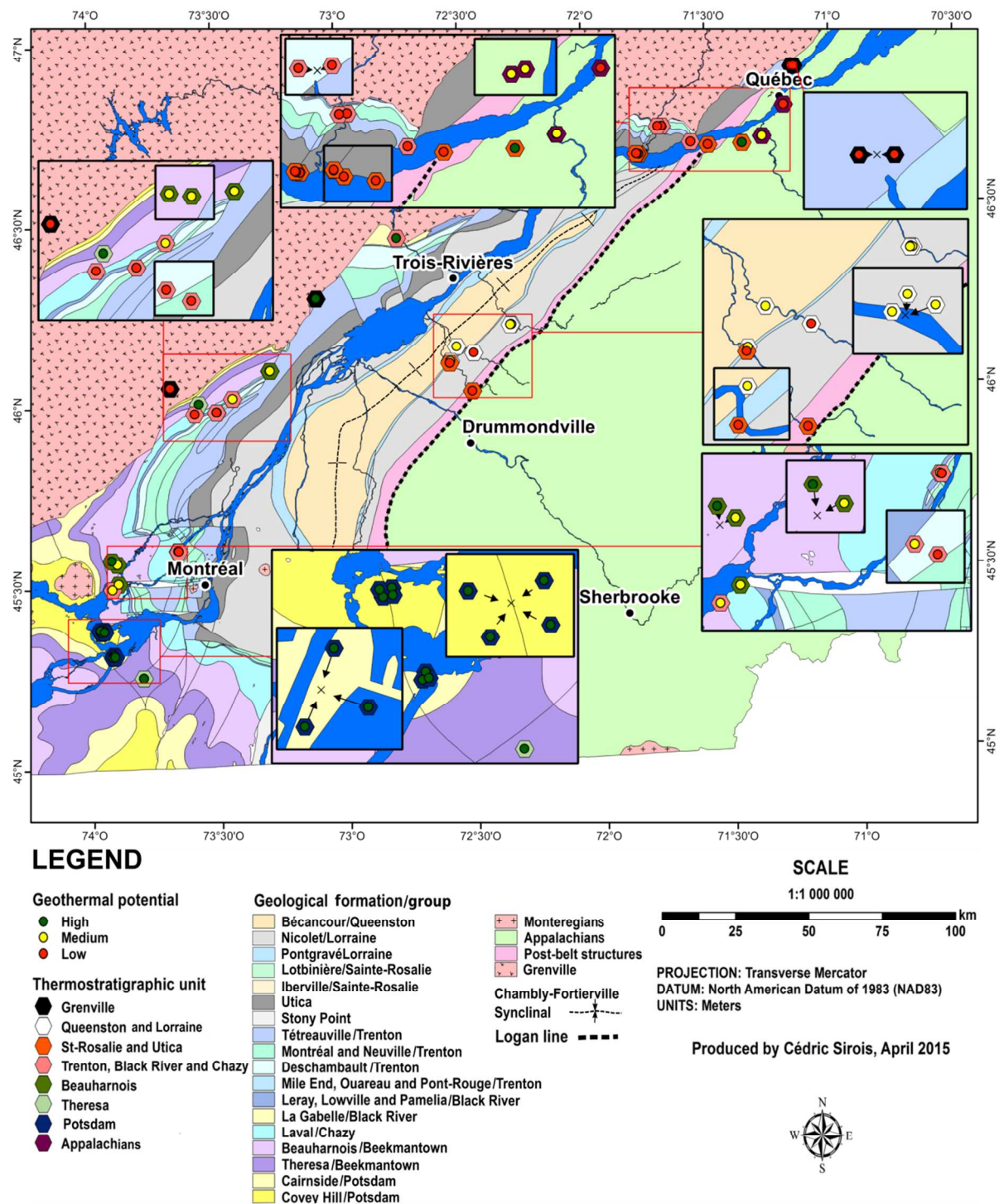


Figure 11. Geothermal heat pump potential of thermostratigraphic units in the St. Lawrence Lowlands (Raymond et al. 2017c).

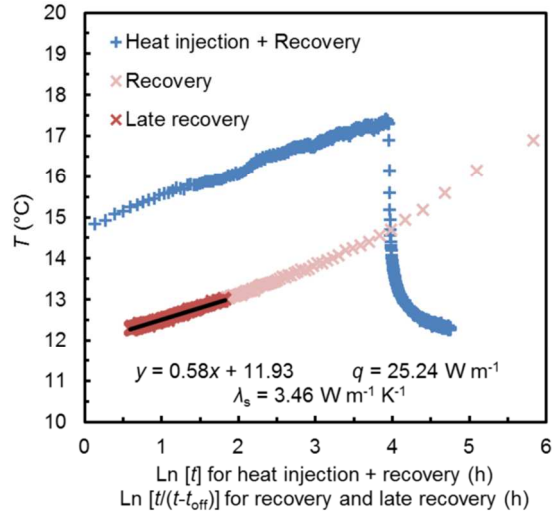


Figure 12. Thermal conductivity analysis at a depth of 18 m for TRT 4 (Table 3), conducted with a continuous heating cable in the Beauharnois Formation.

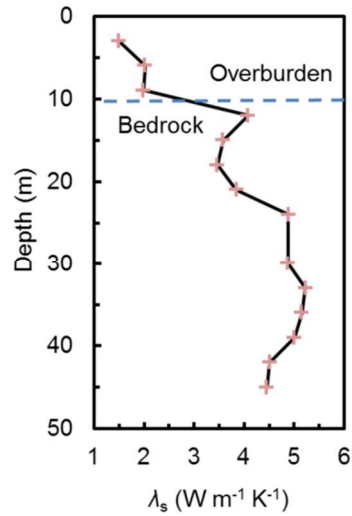


Figure 13. Thermal conductivity profile determined for TRT 4 (Table 3) conducted with a continuous heating cable in the Beauharnois Formation.

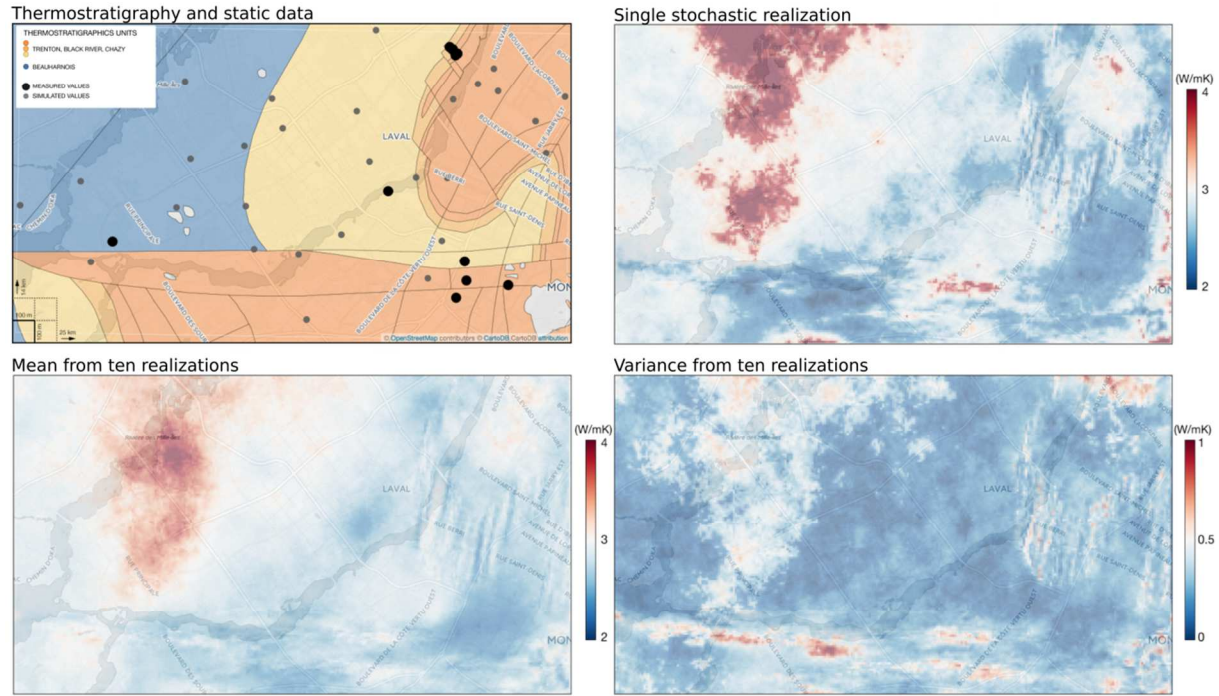


Figure 14. Sequential Gaussian simulations to map the thermal conductivity distribution in an urban district of Montreal (Raymond et al. 2017b).

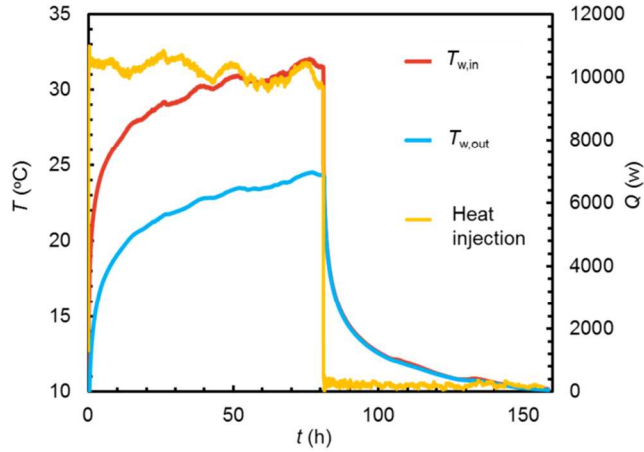


Figure 15. Water temperature and heat injection rate recorded during the conventional TRT at INRS laboratory for a borehole drilled in the Sainte-Rosalie Group.

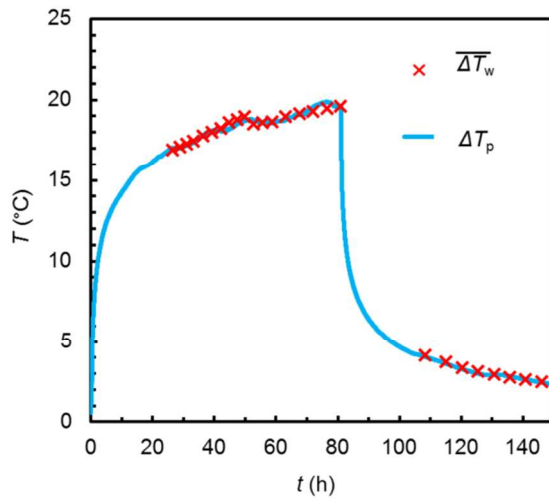


Figure 16. Curve-fitting analysis of conventional TRT at INRS laboratory for a borehole drilled in the Sainte-Rosalie Group.

Table 1. Classification of methods to evaluate the subsurface thermal conductivity in the scope of geothermal heat pump system design.

Method	Mean		Scale		Process		Example
	Active	Passive	Field	Sample	Steady-state	Transient	
TRT Conventional, heat extraction, recovery, distributed, heating cable, constant temperature	x		x			x	(Witte et al. 2002; Fujii et al. 2009; Wang et al. 2010; Rainieri et al. 2011; Raymond et al. 2011b, 2015a)
Geophysical well log		x	x		N.A.	N.A.	(Alonso-Sánchez et al. 2012)
Temperature profile		x	x		x	x	(Rohner et al. 2005; Raymond et al. 2016)
Divided bar	x			x	x		(Barry-Macaulay et al. 2013)
Needle Probe	x			x		x	(Barry-Macaulay et al. 2013; Di Sipio et al. 2014; Luo et al. 2016a; Raymond et al. 2017c)
Plane source	x			x		x	(Di Sipio et al. 2014)

Table 2. Design parameters used for sizing calculations in the St. Lawrence Lowlands (Raymond et al. 2017c).

Parameter	Unit	Value
Peak hourly ground load (Q_{6h})	W	-7500
Monthly ground load (Q_{1m})	W	-3750
Yearly average ground load (Q_{10y})	W	-998
Undisturbed subsurface temperature (T_0)	°C	8
Fluid heat capacity (c_w)	J kg ⁻¹ K ⁻¹	3930
Total mass flow rate per W of peak hourly ground load ($Q' \rho_w Q_{6h}^{-1}$)	kg s ⁻¹ W ⁻¹	78
Minimum heat pump inlet temperature ($T_{w,o}$)	°C	-2
Borehole thermal resistance (R_b)	m K W ⁻¹	0.082-0.087

Table 3. Thermal conductivity measurements used for geostatistical simulations over an urban district (Raymond et al. 2017b).

Latitude UTM NAD 83	Longitude	Thermal conductivity W m ⁻¹ K ⁻¹	Method	Thermostratigraphic unit
45.519249	-73.652824	2.10	Laboratory: MTPS 1	Trenton, Black River, Chazy
45.519249	-73.652824	2.22	Laboratory: MTPS 2	Trenton, Black River, Chazy
45.547637	-73.696752	2.90	Laboratory: MTPS 3	Trenton, Black River, Chazy
45.603070	-73.656963	2.90	Laboratory: MTPS 4	Trenton, Black River, Chazy
45.604803	-73.659649	3.15	Laboratory: MTPS 5	Trenton, Black River, Chazy
45.605735	-73.661411	2.31	Laboratory: MTPS 6	Trenton, Black River, Chazy
45.603070	-73.656963	2.60	Laboratory: MTPS 7	Trenton, Black River, Chazy
45.602381	-73.658056	2.93	Laboratory: MTPS 8	Trenton, Black River, Chazy
45.509640	-73.627682	2.24	Laboratory: MTPS 9	Trenton, Black River, Chazy
45.604803	-73.659649	2.16	Laboratory: MTPS 10	Trenton, Black River, Chazy
45.511454	-73.651800	2.39	Field: TRT 1	Trenton, Black River, Chazy
45.504581	-73.657720	2.39	Field: TRT 2	Trenton, Black River, Chazy
45.516988	-73.648486	2.81	Field: TRT 3	Trenton, Black River, Chazy
45.527392	-73.855424	4.20	Field: TRT 4	Beauharnois